

AD 607491

✓
AFCR: 64-755

THE MINERAL INDUSTRIES EXPERIMENT STATION

College of Mineral Industries

THE PENNSYLVANIA STATE UNIVERSITY

Department of Geology and Geophysics

Special Technical Report on an Estimation Procedure
for Focal-Depth Determination of Seismic Disturbances

by

Stephen C. Merdler

September 8, 1964

AIR FORCE CAMBRIDGE
RESEARCH LABORATORIES
OFFICE OF AEROSPACE RESEARCH
UNITED STATES AIR FORCE
BEDFORD, MASSACHUSETTS
Contract AF19(628)-238 ✓
Project 8652, Task 865208

ADVANCED RESEARCH
PROJECTS AGENCY
PROJECT VELA-UNIFORM
ORDER 292, AMENDMENT 12
PROJECT CODE 4810, TASK 2

COPY	2	OF	3	1/2 p
HARD COPY	\$ 4.00			
MICROFICHE	\$ 0.75			



114p
DDC
RECEIVED
NOV 2 1964
DDC-IRA C

University Park, Pennsylvania

**BEST
AVAILABLE COPY**

PENNSYLVANIA'S COLLEGE OF MINERAL INDUSTRIES

FIELDS OF WORK

Earth Sciences

Geology - Mineralogy - Geophysics - Geochemistry - Meteorology - Geography

Mineral Engineering

Mineral Economics - Mining - Mineral Preparation - Petroleum and Natural Gas

Mineral Technology

Ceramic Technology - Fuel Technology - Metallurgy

Analytical and Structural Studies

Silicate and Carbonate Rock Analysis - X-ray Crystallography

Electron Microscopy and Diffraction - Instrumental Analysis

Requests for additional copies of this report by agencies of the Department of Defense, their contractors, or other government agencies should be directed to:

DEFENSE DOCUMENTATION CENTER (DDC)
CAMERON STATION
ALEXANDRIA, VIRGINIA 22314

Department of Defense contractors must be established for DDC services or have their "need-to-know" certified by the cognizant military agency of their project or contract.

All other persons and organizations should apply to the:

U. S. DEPARTMENT OF COMMERCE
OFFICE OF TECHNICAL SERVICES
WASHINGTON, D. C. 20230

STUDIES OF THE EFFECT OF DEPTH OF FOCUS
ON SEISMIC PULSES

B. F. Howell, Jr. (814-865-6821)
P. M. Lavin (814-865-2622)
R. J. Watson (814-865-2622)

The Pennsylvania State University
Department of Geology and Geophysics
Mineral Sciences Building
University Park, Pennsylvania

Special Technical Report on an Estimation Procedure
for Focal-Depth Determination of Seismic Disturbances

by

Stephen C. Merdler

September 8, 1964

Contract AF19(628)-238

Prepared

for

AIR FORCE CAMBRIDGE RESEARCH LABORATORIES
OFFICE OF AEROSPACE RESEARCH
UNITED STATES AIR FORCE
BEDFORD, MASSACHUSETTS

WORK SPONSORED BY ADVANCED RESEARCH PROJECTS AGENCY
PROJECT VELA-UNIFORM

ARPA Order No. 292, Amendment 12
Project Code No. 4810, Task 2

ABSTRACT

A new data processing technique is suggested to estimate the delay time between initially uptraveling energy which is reflected once at the earth's surface and initially downtraveling energy on earthquake seismograms. The method uses optimum inverse filter together with a criterion that measures the simplicity of a seismic signal convolved with an inverse filter. The inverse filters are designed to extract primary energy in the presence of surface reflected energy and random noise on the basis of a least-mean-square error criterion. Filter design is dependent on the delay time between primaries and surface reflected events, their amplitude ratio and noise to signal power ratio. The simplicity criterion was devised on the assumption that a maximum in the concentration of normalized seismic signal energy above a minimum level indicates which filter was most correctly designed. This is visualized as an expression of the hypothesis that the primary seismogram is generated by a few large discontinuities, rather than by many minor boundaries.

The technique was applied to band-limited synthetic signals that contained several primary-secondary pairs in the presence of random noise. Of 27 synthetic signals which were analyzed, the procedure successfully selected the correct delay time in 22 cases.

Four actual earthquake seismograms were then analyzed. The procedure selected a delay time for each earthquake. Focal depths computed from the selected delay times appeared quite reasonable when

compared with depths for the same earthquakes published by the United States Coast and Geodetic Survey. In all cases, the inverse filter designed for the selected delay time considerably simplified the original seismogram.

It is concluded that the technique provides a reasonable estimate of the delay time between primary and surface reflected energy.

ACKNOWLEDGEMENTS

The author wishes to express his appreciation to Dr. R. J. Watson for his invaluable guidance throughout all phases of this study and to Drs. B. F. Howell and P. M. Lavin for their helpful discussions.

This work was supported by The Pennsylvania State University Computer Center and in part by Contract AF19(628)-238 of the Air Force Cambridge Research Laboratories as part of the advanced Research Projects Agency VELA UNIFORM program.

TABLE OF CONTENTS

	<u>Page</u>
Abstract	ii
Acknowledgement	iv
List of Tables	vi
List of Figures	vii
 I. INTRODUCTION	
General statement of the problem	1
Previous studies	2
Explanation of the suggested procedure	7
Mathematical model for the present study	9
Focal depth estimation procedure	12
Theoretical design of the inverse operators	14
Primary-estimation method	21
Conversion of T into focal depth	24
Scope and limitations of study	26
 II. PROCEDURE OF THE INVESTIGATION	
Design of the optimum inverse filters	28
Synthetic signals	29
Construction of the travel-time curves	34
 III. EXPERIMENTAL RESULTS	
Single doublet function	37
Bandlimited single doublet functions	39
Bandlimited triple doublet functions	40
Synthetic signals for a 2.5 km focal depth	42
Synthetic signals for a 5.0 km focal depth	45
Synthetic signals for a 10.0 km focal depth	48
Analysis of earthquake seismograms	48
 IV. SUMMARY AND CONCLUSIONS	
APPENDIX A. Proof of simplicity criterion for doublet function with no noise and perfect inverse	61
APPENDIX B. Optimum inverse filters designed for the doublet function	65
APPENDIX C. Fortran computer programs	72
REFERENCES	92

LIST OF TABLES

<u>Table</u>		<u>Page</u>
1	Values for delay time (T), ghost amplitude (R_0) and noise to signal power ratio (R) used to construct synthetic seismograms	31
2	Values for twelve 20-point inverse operators for the doublet function designed for a 0.01 noise to signal power ratio	67
3	Values for twelve 20-point inverse operators for the doublet function designed for a 0.0625 noise to signal power ratio	69
4	Values for twelve 20-point inverse operators for the doublet function designed for a 0.25 noise to signal power ratio	71

LIST OF FIGURES

<u>Figure</u>		<u>Page</u>
1	Gutenberg and Richter ray-path configuration	3
2	Thirlaway's ray-path configuration for crustal earthquakes recorded in the first zone	3
3	Schematic of the proposed data generation hypothesis .	12
4	Schematic of the proposed focal depth estimation procedure	14
5	Flow chart for formulation of the optimum inverse filter problem	15
6	Flow chart of problem for finding an optimum inverse filter for the doublet function	17
7	Output signal $z(t)$ found by convolution of $h^{-1}(t)$ (correct inverse) with the input signal $h(t)$	18
8a	One period of the amplitude spectra of the ghost filter, ghost inverse and their product	20
8b	Spectrum of input signal before inverse filtering . .	20
8c	Spectrum of input signal after inverse filtering . . .	20
9	Output signal $z(t)$ found by convolution of $h^{-1}(t)$ (incorrect inverse) with the input signal $h(t)$	21
10	Diagram of the parameters involved in the formulation of the simplicity criterion	22
11	Parameters involved in constructing travel-time curves for P and pP	26
12a	Crustal layering used to generate synthetic spike seismograms	30
12b	Synthetic spike seismograms for three focal depths . .	30
13	Impulse and frequency response curves for the Benioff Geneva-type seismometer system	32
14	Evaluation procedure for synthetic signals	33
15	Travel-time curves for P-pP derived from a piecewise continuous velocity function	36

<u>Figure</u>		<u>Page</u>
16	Results of estimation procedure applied to a single doublet function	38
17	Simplicity criterion used to determine the correct ghost delay time for three band-limited doublet functions containing random noise	41
18	Synthetic signals $S(t)$ for a 2.5 km focal depth (0.3 sec delay time) with their deghosted signals $\hat{P}(t)$ selected by the simplicity criterion	43
19	Energy concentration ($c(T)$) versus delay time for synthetic signals generated for a 2.5 km focal depth	44
20	Synthetic signals $S(t)$ for a 5.0 km focal depth (0.9 sec delay time) with their deghosted signals selected by the simplicity criterion	46
21	Energy concentration ($c(T)$) versus delay time for synthetic signals generated for a 5.0 km focal depth	47
22	Synthetic signals $S(t)$ for a 10.0 km focal depth (1.6 sec delay time) with their deghosted signals $\hat{P}(t)$ selected by the simplicity criterion	49
23	Energy concentration ($c(T)$) versus delay time for synthetic signals generated for a 10.0 km focal depth	50
24	Input earthquake seismograms and their deghosted counterpart selected by the simplicity criterion	52
25	Energy concentration ($c(T)$) versus delay time for earthquake seismograms	53
26	Graphs summarizing the T, R selection capability of the estimation procedure for the synthetic signals	58
27	Parameters involved in proof of simplicity criterion for doublet function with no noise and perfect inverse	62
28	Diagrams of twelve 20-point inverse operators designed for the doublet function for $R = 0.01$	66
29	Diagrams of twelve 20-point inverse operators designed for the doublet function for $R = 0.0625$	68
30	Diagrams of twelve 20-point inverse operators designed for the doublet function for $R = 0.25$	70

INTRODUCTION

General Statement of the Problem

This thesis is concerned with the problem of extracting information from a bandlimited signal in the presence of corrupting noise. In particular the signal is a seismic signal generated by an earthquake at or near the earth's surface. The information desired is a correct estimate of the focal depth of the earthquake's source.

An accurate estimate of the source depth would help to differentiate natural earthquakes from clandestine nuclear explosions, since the depth of a nuclear explosion is subject to practical limitations. For example, all disturbances with focal depths greater than say 10 km could be classified as natural with reasonable certainty.

The Coast and Geodetic Survey is the agency in the United States which routinely collects seismic data from stations throughout the world. They compute the focal depth of an earthquake in kilometers below the mean sphere based on P-arrivals and on the Jeffreys-Bullen travel-time tables of 1958. The survey made the following statement concerning the accuracy of their published focal depths.

"A freely determined depth is checked against depth phases interpreted from available seismograms or reported by cooperating observatories. Depths may be restricted to agree with these depth phases if agreement to within the stated accuracy is not obtained. In the case of shallow earthquakes or smaller earthquakes, the exact depth cannot usually be determined precisely and the depths quoted represent a judgment." (U. S. Department of Commerce Coast and Geodetic Survey, 1964)

A focal depth for an earthquake published by this survey may be in error by as much as 25 kilometers. (Ganst and Engdahl, 1962).

Previous Studies

Several investigators have tried with varying degrees of success to develop techniques that will obtain more accurate focal depths from seismograms. Most techniques or suggested methods fall in one of three categories: visual recognition of seismic events with arrival times related to focal depth, spectral analyses and linear filter operations.

Visual recognition is the most obvious technique and simplest to apply. In 1936 Gutenberg and Richter suggested using visible and clearly identifiable pulses such as P, S and pP (Howell, 1959). The paths followed by these pulses are illustrated in Figure 1. S-waves follow essentially the same path as P-waves but at a slower velocity. If the velocity profile at the source is known, the delay time (difference in arrival times) between pP and P gives a direct estimate of the focal depth. A knowledge of the epicentral distance and time of origin of the event, combined with arrival times for P and S, also gives a direct estimate of the depth of focus. For shallow earthquakes sP may be easier to identify than pP. This is due to the fact that sP travels to the surface at a slower velocity than pP, and hence is separated by a greater time difference from P. Kondorskaya (1956) has in some cases identified sP and used its arrival time to determine the focal depth of a shallow event.

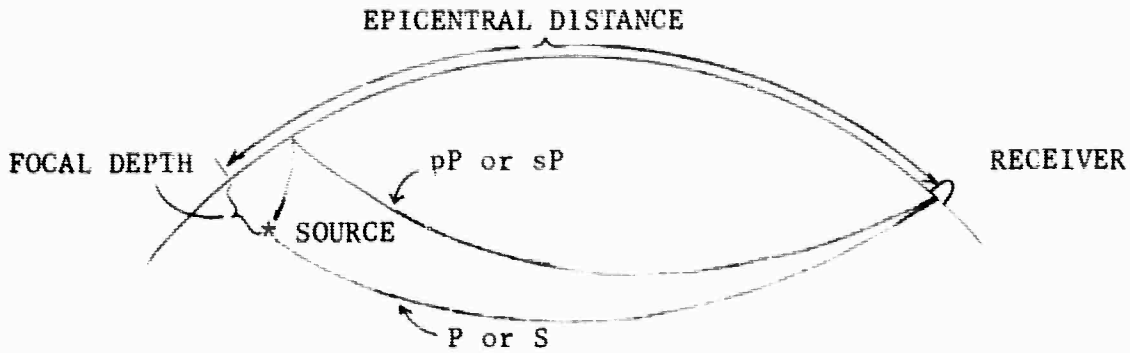


Fig. 1. Gutenberg and Richter ray-path configuration.

For crustal earthquakes other pulses may be used provided that the receiving station is at a distance (D) from the source that lies within the first zone. This zone includes distances up to 1000 kilometers, for which the curvature of the earth can be neglected. When this is the case, (i.e., D is known and $D < 1000$ km) Thirlaway (1961) suggests using the delay time between P_g and P_n or S_g and S_n to determine the focal depth. The ray-paths for these pulses are illustrated in Figure 2. De Bremaeker (1955) has shown that the variation of P_n amplitude with epicentral distance is also related to the source depth of crustal earthquakes.

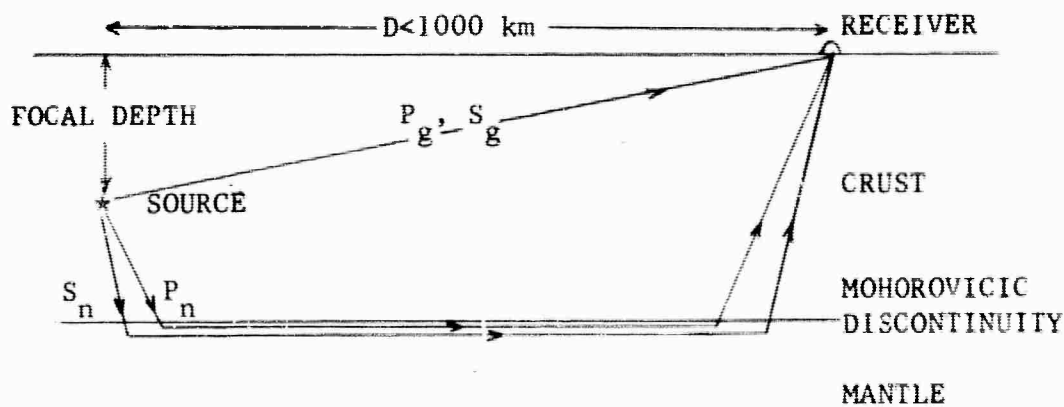


Fig. 2. Thirlaway's ray-path configuration for crustal earthquakes recorded in the first zone.

All these techniques depend on visual identification of clearly recognizable pulses. This is a severe restriction when focal depths are shallow and consequently differences in arrival time are so small that pulses overlap. Furthermore background noise level impairs visual identification.

As an alternative to direct visual recognition of seismic events, correlation procedures have also been suggested. Time autocorrelation of the seismic signal was used by The California Research Corporation (Cal. Research) (1961) and Rothman (1964) to estimate the delay time between two sets of pulses whose time separation is related to the source depth. This process measures the correlation of the signal as a function of time as it is shifted across itself. Mathematically this is expressed as

$$\varphi(T) = \int_{-\infty}^{+\infty} x(t+T)x(t)dt$$

where $\varphi(T)$ is the time-autocorrelation function, and T is the time displacement (shift) of $x(t)$ (Lee, 1963). The maximum correlation occurs when $T = 0$ and is positive. For a seismic signal containing two pulses or two sets of pulses having the same shape but differing in amplitude, there will be a relative maximum in the absolute value of $\varphi(T)$ at T equal to their time separation. If the pulse sets have the same polarity this correlation will be positive, and if they have opposite polarities it will be negative. When more than two pulse sets are included in the analysis, other correlation peaks or troughs will appear in the function. If this is the case, the position of the relative maximum may or may not correspond to the correct delay time.

The difference frequency between minima in the amplitude spectrum of a transient containing two pulses or two functions of the same shape, has been shown by Nakamura (1963) to be related to their delay time. When the pulses are out of phase Nakamura showed that minima in the spectrum will appear at integer multiples of the harmonic frequency given by

$$F_0 = \frac{1}{T}$$

where T is the time separation of the two pulses.

Rothman (1964) obtained spectra for two-dimensional model records, and was successful in picking the difference frequency related to the focal depth when the duration of analysis included only the two pulses of interest. Some ambiguity in picking the correct difference frequency resulted when more pulses were included in the analysis. That is, the difference frequency does not uniquely determine the delay between two pulses unless they are the only major pulses in the signal.

Bogert et al (1963) used the time autocorrelation function of a seismic signal to find the Cepstrum. They defined the Cepstrum to be the spectrum of the log-power spectrum. By band-broadening the log-power spectrum of the autocorrelation function they found that they could sometimes locate periodicities (related to the delay time) in the Cepstrum that were not evident in the autocorrelation function. Their results were quite dependent on the type of high-pass filter they used for band-broadening the log-power spectrum.

Both Keylis Borok (1962) and Cal. Research (1961) used the amplitude spectrum of surface waves to differentiate between earthquakes and nuclear explosions. Energy distribution as a function of frequency actually depends on several factors, one of which is the source depth. However, more predominant factors such as detector location, earth layering and source-detector separation are more important in determining the frequency distribution of energy, thus limiting the power of this technique.

To be successful most of these procedures can only be applied to relatively broad-band signals. However, seismic signals are inherently narrow-band (2-3 octaves). This is because the amount of attenuation of seismic energy due to absorption (earth filtering) is frequency dependent. The result of this is a rapid loss of high-frequency energy in seismic waves with distance from the source (Howell, 1959). In addition, the instrumentation at the receiver and the local geology at both the source and receiver tend to limit the bandwidth of seismic energy.

Recognition of these facts has stimulated researchers to attempt to band-broaden seismic data. Sufficient band-broadening should visually simplify a seismic signal and help to make individual pulses recognizable. At the Massachusetts Institute of Technology under the direction of Simpson (1961, 1962) and Cal. Research (1961), research has been directed towards finding an estimate of the earth filter. Convolution of the inverse of the earth filter with the seismic signal should yield a broader-band signal. Scientific reports from M.I.T. (Simpson, 1961, 1962) and Cal. Research (1961) suggest that

the shape of the first primary pulse in a seismic signal would be a reasonably good estimate of the earth filter. However, seismograms filtered with the inverse of the primary pulse were not significantly simplified. This inability to simplify the seismogram with inverse filtering of the earth filter is due to several reasons. In the first place, the process for finding the inverse filter is extremely sensitive to truncation or smoothing of the original pulse shape (Watson, 1964 personal communication). Furthermore, it is very difficult to obtain a good estimate of the earth filter from the seismic signal, due to corrupting noise and overlapping pulses. Even if the earth filter were known reliably it is doubtful that much band-broadening could be achieved, due to the presence of noise and the limited bandwidth of the seismic filter (Howell et al, 1953).

Due to the problems inherent in the application of many of the techniques just discussed, it is apparent that a new approach to the focal depth problem is necessary. In the following pages we will investigate a new technique that circumvents many of the difficulties discussed in this section.

Explanation of the Suggested Procedure

Let us consider a seismic disturbance at some arbitrary depth beneath the earth's surface. The disturbance emanates energy in all directions. Energy sent initially downward travels directly, as well as through a combination of refractions and reflections, to a receiver. At the receiver this energy creates a series of pulses on the seismogram which we call primary events. Energy emanated initially upward is

reflected at the earth's surface (or from intermediate discontinuities), and then follows travel paths to the receiver similar to those taken by the initially downward-traveling energy. This energy also creates a series of pulses on the seismogram which we call secondary events or ghosts. In addition, other events such as surface waves and microseisms are recorded. These events and all others which are neither primaries nor ghosts constitute noise in this mathematical model (Howell et al, 1963).

Let us suppose that each primary event has an associated ghost. This ghost is presumed to have the same pulse shape as the primary but is reversed in polarity. The ratio of ghost to primary amplitude (R_0) is determined primarily by the surface reflection coefficient, and attenuation of ghost energy in its longer travel path. Due to its longer travel path, the ghost lags behind the primary by a time I dependent on the depth of the disturbance.

Now if we could design an operator* that could suppress the secondary events on a seismogram (inverse filtering), only the primary events would remain in the presence of filtered noise. Presumably the best operator would be designed with an exact knowledge of I and R_0 . If it be effective it would also have to operate in the presence of corrupting noise. However, I and R_0 in general would not be known. If I were known there would be no problem. But if several inverse operators were designed covering the range of possible values of R_0 and I , one of these would be most nearly correct, at least to within the intervals of variation chosen for R_0 and I . To ascertain which inverse

* Operator and filter will be used as synonyms in this paper.

operator based on particular values of R_0 and I was correct, it would be necessary to determine which inverse filtered seismogram most nearly contains only primary events. A criterion which attempts to measure the simplicity of the inverse filtered seismogram could be devised to make the latter determination. The primary-ghost separation would then be known and hence the depth of the source could be obtained, if the velocity profile were known.

The procedure just outlined would not require a knowledge of the earth filter. Further, it should be reasonably independent of the number of primary-ghost pairs provided that the pulse shape of each ghost is the same as its associated primary, and that their amplitude ratio is the same for all pairs included in the analysis.

Mathematical Model for the Present Study

Mathematically the above ideas may be expressed as follows. Let the pulse shape of the events that initially traveled downward be $b(t)$. In this model, $b(t)$ includes the shot generation pulse, the earth transmission attenuation characteristic and the filtering due to recording instrumentation. It is equivalent to the $b(t)$ function as defined by Sengbush et al (1961) with additional filtering due to attenuation. By writing $b(t)$ instead of $b(t, I)$, where I is travel time, we have assumed time-invariance of the seismic wavelet, and thus have asserted that the attenuation is identical for all events on a given seismogram. By defining $b(t)$ in this way the primary events on the seismogram may be expressed as,

$$P(t) = b(t)*r(t) \quad (1)$$

(Simpson, 1961), where $r(t)$ is the response of the earth to a plane-wave impulsive source propagating without attenuation and recorded with perfect instruments. $r(t)$ includes the direct pulses (for teleseismic events), reflections and refractions which have ghost counterparts. All other events not having ghost counterparts such as surface waves are considered part of the noise. This $r(t)$ is analogous to the "reflectivity function" introduced by Peterson et al (1955) which is restricted in their model to include only reflected events. The asterisk "*" stands for convolution

$$x(t)*y(t) = \int_{-\infty}^{+\infty} x(T)y(t-T)dT. \quad (2)$$

If we consider only those ghosts which reflected from the earth's surface (these are believed to contain the most energy), then the secondary events may be expressed by

$$G(t) = -R_0 b(t-T)*r(t). \quad (3)$$

Here R_0 is the ratio of ghost to primary amplitude and may range from almost zero to slightly greater than unity in magnitude. T is the time required for energy to travel to the earth's surface from the source, and back down again to the same depth as the disturbance.

The expression for the recorded signal is the sum of the primary (equation (1)), and secondary (equation (3)) events together with noise,

$$S(t) = P(t)+G(t)+n(t). \quad (4)$$

Noise, $n(t)$, constitutes all other events which are neither primaries nor ghosts. Rewriting (4) we have,

$$S(t) = b(t) * r(t) - R_0 b(t-T) * r(t) + n(t). \quad (5)$$

This may be written,

$$S(t) = b(t) * r(t) * [\delta(t) - R_0 \delta(t-T)] + n(t). \quad (6)$$

$\delta(t)$ is the impulse function

$$\begin{aligned} \delta(t) &= 0 & t \neq 0 \\ \int_{-\infty}^{+\infty} \delta(t) dt &= 1 & t = 0 \end{aligned}$$

(Churchill, 1958). $\delta(t)$ has the additional property that

$$\delta(t) * y(t) = y(t).$$

Now let

$$h(t) = \delta(t) - R_0 \delta(t-T). \quad (7)$$

$h(t)$ is a doublet function consisting of two impulses, one positive and the other negative, and separated in time by an amount T . R_0 is the ratio of their amplitudes. This doublet function will be called the ghost filter. Substituting for $h(t)$ in (6), we have,

$$S(t) = b(t) * r(t) * h(t) + n(t) \quad (8)$$

$S(t)$ in (8) is the proposed mathematical expression for the recorded sequence of events generated by a source at an arbitrary depth beneath the earth's surface. Figure 3 is a schematic of the proposed data

generation process.

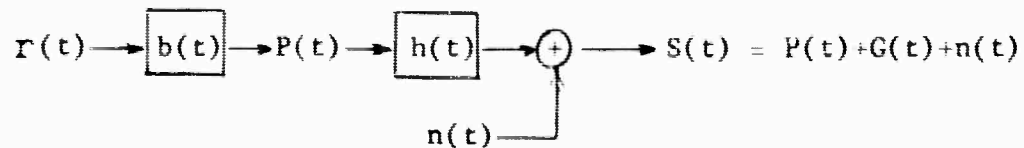


Fig. 3. Schematic of the proposed data generation hypothesis.

In summary the data generation hypothesis is based on the following assumptions. All primary events generated by a seismic disturbance pass through a ghost filter. This filter introduces a pulse (ghost) after each primary that has the same pulse shape as the primary but is reversed in polarity. It is delayed by a time that is related to the depth of the disturbance. The amplitude ratio of the primary to ghost is fixed for all primary-ghost pairs on a given seismogram. All other events which are neither primaries nor ghosts constitute noise.

Focal Depth Estimation Procedure

Suppose R_0 and T are known, then $h(t)$ is completely specified. Now devise an operator $h^{-1}(t)$ which has the property

$$h^{-1}(t) * h(t) \approx \delta(t). \quad (9)$$

This is an approximation since $h^{-1}(t)$ must be designed to extract the primary events from a signal in the presence of noise, and hence a perfect inverse operator or exact inverse is not required (Foster et al, 1962). It follows that,

$$\begin{aligned}
h^{-1}(t)*S(t) &= h^{-1}(t)*b(t)*r(t)*h(t) + n'(t) \\
&\approx b(t)*r(t) + n'(t) \\
&\approx P(t) + n'(t)
\end{aligned}
\tag{10}$$

where $n'(t) = h^{-1}(t)*n(t)$. $h^{-1}(t)$ is the mathematical inverse of $h(t)$, a doublet function in the sense to be described under Theoretical Design of Inverse Operators. The design of $h^{-1}(t)$ requires a knowledge of R_0 and T . Since in general, knowledge of these parameters will be limited, it is suggested that an array of inverse operators $h^{-1}(t, R_{0j}, T_k)$ be generated for various values of R_0 and T . The j and k subscripts on R_{0j} and T_k refer to possible values of the R_0 and T parameters.

The given earthquake seismogram is filtered by each of these inverse operators (Figure 4) producing a suite of inverse filtered traces P_{jk} , each for a different R_{0j}, T_k combination in the inverse filter. That combination of R_{0j} and T_k for the inverse filter which yields the "best" estimate of the primaries is considered the most correct combination for the signal analyzed. By "best" we mean that set of primaries whose energy is concentrated in the fewest number of large pulses. This set of primaries relative to the other sets should have the simplest structure. The simplicity criterion is an attempt to quantify this concept. This criterion will yield an estimate of T and R_0 , called \hat{T} and \hat{R}_0 . \hat{T} together with an appropriate velocity profile will be used to estimate the depth of focus of the earthquake. The complete estimation procedure is illustrated schematically in Figure 4.

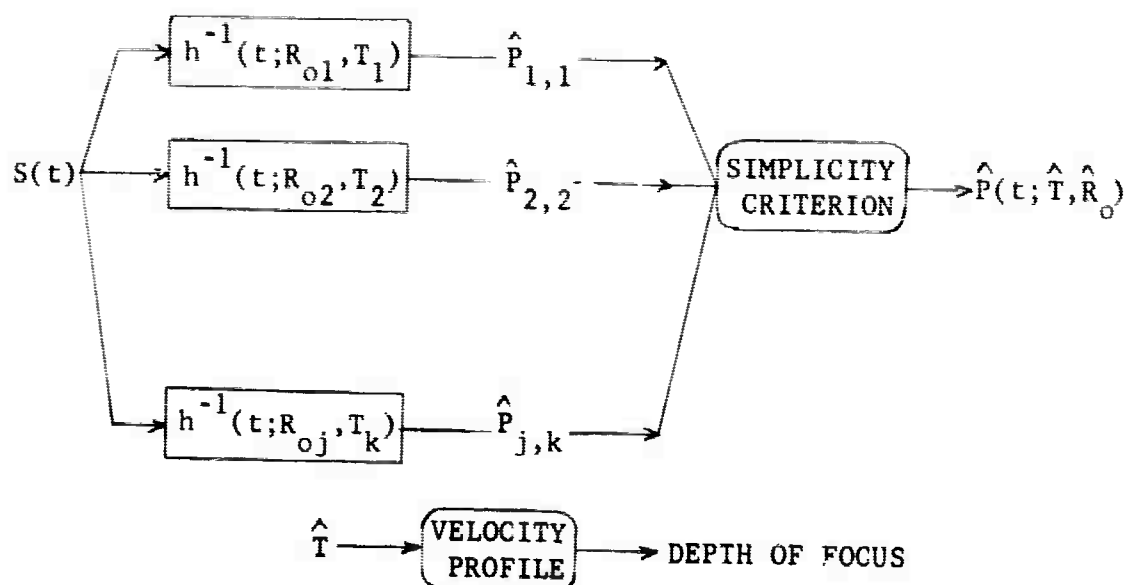


Fig. 4. Schematic of the proposed focal depth estimation procedure.

Theoretical Design of the Inverse Operators: An expression for the exact inverse operator for the doublet function $h(t)$ was derived by Lindsey (1960), and has the form,

$$h^{-1}(t; R_o, T) = \sum_{n=0}^{\infty} R_o^n \delta(t-nT).$$

This expression for $h^{-1}(t)$ is neither practical nor desirable. First of all, it requires an infinite number of points and secondly, it is inadequate for a system containing noise. The inverse filter we require should be capable of doing an effective job in the presence of noise. It should also contain only a finite number of points so that it may be used in a computer.

The general technique for designing an optimum filter was developed by Norbert Wiener (1949). He formulated a criterion or least-

square measure that gave an objective indication of filter performance. An optimum filter is a filter which minimizes the mean-square error difference between a desired output and the actual output of the filter as explained below. In addition, Wiener statistically described the signal and noise.

The procedure for finding the optimum inverse filter was outlined by Foster et al (1962). The problem was formulated in the manner indicated by the flow chart in Figure 5.

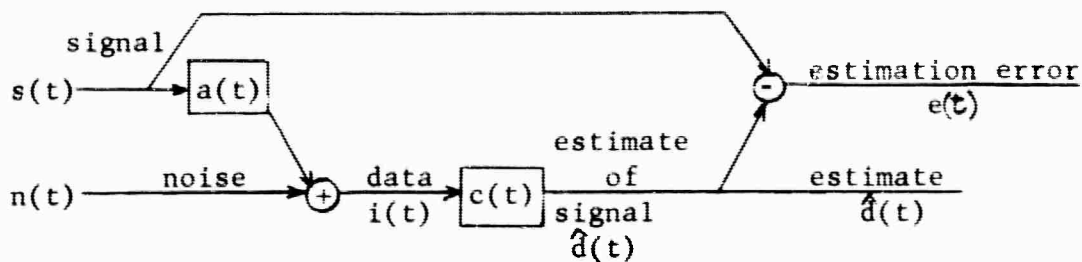


Fig. 5. Flow chart for formulation of the optimum inverse filter problem.

The purpose was to determine $c(t)$ which is in a certain sense the inverse to the filter labeled $a(t)$. $c(t)$ is restricted to be a linear, band-limited, time-invariant, finite memory filter. The data that $c(t)$ operates upon is the filtered signal mixed with noise

$$i(t) = \int_{-\infty}^{+\infty} a(t) s(t-T) dT + n(t). \quad (11)$$

The output of $c(t)$ is an estimate of $s(t)$ and is given by

$$\hat{d}(t) = \int_{-\infty}^{+\infty} c(t) i(t-T) dT, \quad (12)$$

where " $\hat{}$ " is used to indicate that $\hat{d}(t)$ is an estimate of $s(t)$. The error made in estimating $s(t)$ is

$$e(t) = s(t) - \hat{d}(t). \quad (13)$$

According to Wiener (1949) the best estimate $\hat{d}(t)$ of $s(t)$ is obtained when a filter $c(t)$ is used that minimizes the mean-square error. The mean-square error in this case is given by

$$\lim_{T \rightarrow \infty} \frac{1}{2T} \int_{-T}^T [e(t)]^2 dt. \quad (14)$$

For the case when only a minimum knowledge about the statistical properties of the signal and noise is available (maximum entropy case) Foster made the following assumptions:

1. The signal $s(t)$ and noise $n(t)$ are uncorrelated random processes.
2. The autocorrelation function of $s(t)$ is

$$\psi_s(T) = G_s^2 \delta(T),$$

and for $n(t)$ (15)

$$\psi_n(T) = G_n^2 \delta(T).$$

G_s^2 is the signal power and G_n^2 is the noise power.

The ratio G_n^2/G_s^2 is called the noise/signal power ratio (R).

Using these assumptions Foster derives a stable optimum inverse filter $c(t)$ that minimizes the Wiener mean-square error. $c(t)$ was chosen from the class of all band-limited, finite memory functions.

Using Foster's procedure an optimum inverse filter can be derived for the doublet function $h(t)$ for any combination of R_{oj} , T_k . For this case the flow chart of the problem is illustrated in Figure 6. Here we desire an optimum inverse filter $h^{-1}(t)$ that will minimize the mean-square error

$$\lim_{T \rightarrow \infty} \frac{1}{2T} \int_{-T}^T [\delta(t) - z(t)]^2 dt \quad (16)$$

where $z(t)$ is an estimate of the impulse function $\delta(t)$.

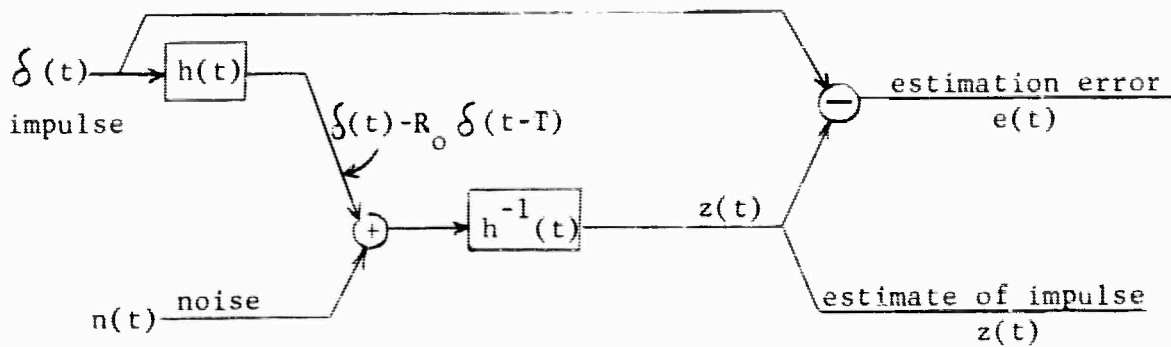


Fig. 6. Flow chart of problem for finding an optimum inverse filter for the doublet function.

In using the Foster model for derivation of the inverse filters, we have assumed that the seismic noise is wide sense stationary and white. These assumptions are probably not true for the seismic data generation process, but are nevertheless appropriate when no further knowledge concerning the noise statistics are available (Foster et al, 1964).

A typical inverse operator together with the input and output signal is shown in Figure 7. The interval between sample points is equal to the assumed delay time between the primary and ghost. Convolution in the time domain with the doublet results in a single positive impulse together with several small negative impulses (secondary spikes). These negative impulses are generated since the inverse operators are only designed to do the best job in the presence of noise, under the finite memory and bandlimit restrictions.

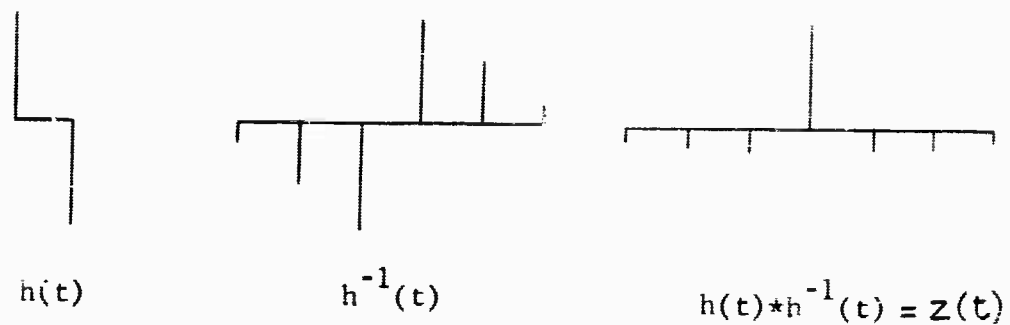


Fig. 7. Output signal $z(t)$ found by convolution of $h^{-1}(t)$ (correct inverse) with the input signal $h(t)$.

Physically the convolution of $h(t)$ with $h^{-1}(t)$ proceeds as follows: The initial impulse in $h(t)$ reproduces $h^{-1}(t)$. The second impulse in $h(t)$, (i.e., $-R_0 \delta(t-T)$) reproduces $h^{-1}(t)$ multiplied by $-R_0$ and delayed T seconds. Thus the second impulse produces $-R_0 h^{-1}(t-T)$. Finally, $h^{-1}(t)$ and $-R_0 h^{-1}(t-T)$ are summed to produce the function labeled $h(t) * h^{-1}(t)$ in Figure 7.

In the frequency domain convolution corresponds to multiplication of spectra. One period of the amplitude spectrum of the ghost filter

$h(t)$ and the amplitude spectrum of the appropriate inverse $h^{-1}(t)$ are shown in Figure 8a. The product of these spectra yields a spectrum that is broader-band than the ghost filter, i.e., more nearly approaches the spectrum of a $\delta(t)$ function).

To examine further the effects of inverse filtering on a signal in the frequency domain, a signal containing three positive impulses (separated in time) was constructed and subsequently filtered to simulate real data.

Figure 8b is the amplitude spectrum of three positive primary impulses that have not been filtered. Below this is the amplitude spectrum of the primaries filtered by the ghost filter and $b(t)$. The next amplitude spectrum in Figure 8c was obtained using the correct inverse filter for the ghost filter. The final spectrum was obtained using an inverse filter designed for a shorter primary-ghost delay time. It is quite clear that this filter boosted both the low and high frequencies in the spectrum. That is, the deconvolved signal using the wrong filter is broader-band than the signal produced by the correct inverse filter. The correct inverse filter did band-broaden the signal but not as much as the incorrect filter. In a few cases, this over-compensation phenomenon is thought to be one reason for the failure of the simplicity criterion to differentiate between two sets of estimated primaries P. This criterion will be explained more fully in the next section.

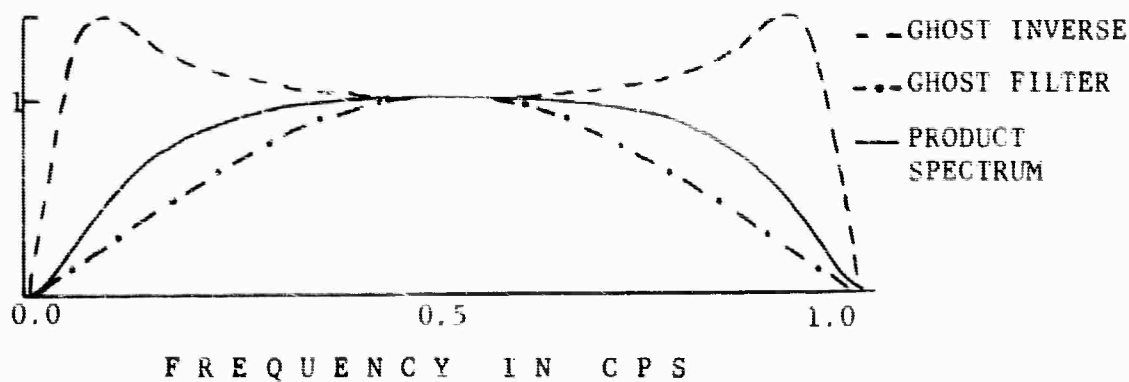


Fig. 8a. One period of the amplitude spectra of the ghost filter, ghost inverse, and their product.

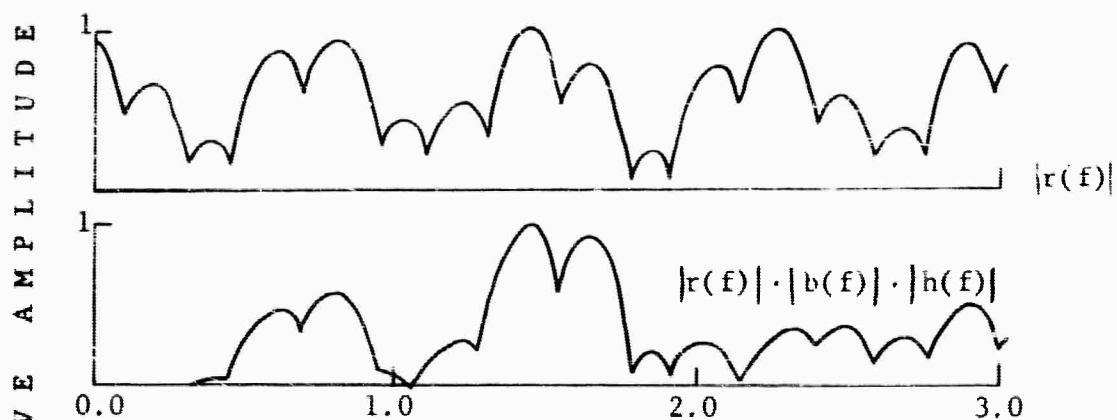


Fig. 8b. Amplitude spectra of input signal before inverse filtering.

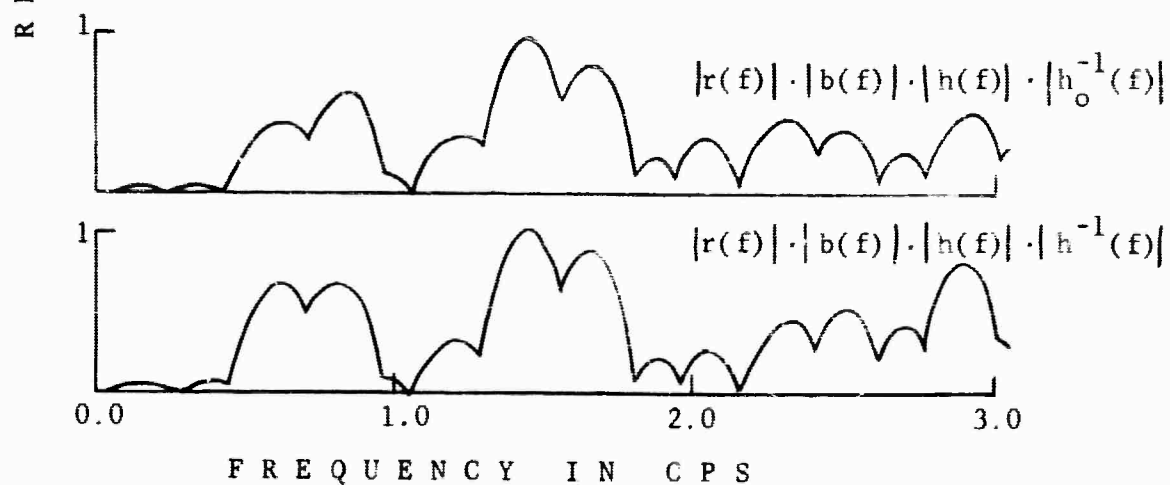


Fig. 8c. Amplitude spectra of input signal after inverse filtering ($h_0^{-1}(f)$ correct inverse, $h^{-1}(f)$ incorrect inverse). The variable f is used to indicate that the functions above are Fourier transforms of time functions. e.g., the Fourier transform of $r(t)$ is designated by $r(f)$.

Primary-estimation Method: Ideally, we would like to choose one of the inverse filtered records as being the best estimate of the primary events $P(t)$. As explained on page 13, this would yield \hat{T} and \hat{R}_0 , estimates of T and R_0 respectively. However, we do not know the actual primary function. Therefore we must use a criterion independent of the true set of primaries to make this choice. We assume that the inverse filtered record (contained in a suite of inverse filtered records) which contained the most nearly correct set of primaries would be the simplest in visual character. Our reasoning here comes from the result of convolution of the actual $h(t)$ filter present in a seismogram, with an $h^{-1}(t)$ filter based on incorrect values for R_0 and T . Figure 9 shows one such possible incorrect $h^{-1}(t)$ convolved with $h(t)$. Comparison of the output of this operation with the desired operation shown in

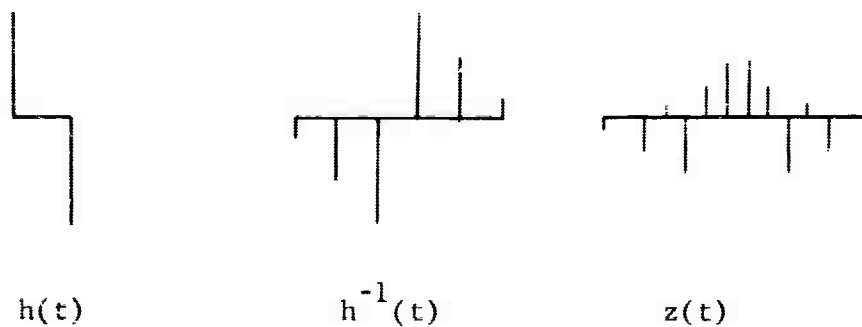


Fig. 9. Output signal $z(t)$ found by convolution of $h^{-1}(t)$ (incorrect inverse) with input signal $h(t)$.

Figure 7 indicates that the correct inverse produces a single large impulse (with attendant small negative spikes) whereas the incorrect inverse produces several large impulses distributed over a longer

time interval. Thus if we can measure the concentration of energy per unit time, i.e., quantify the visual difference between Figures 7 and 9, we would have an objective criterion for choosing the result of Figure 7 over that in Figure 9.

As a measure of energy concentration per unit time we choose the function

$$C(u; R_{oj}, T_k) = \frac{\int_{A_i} (|\hat{P}(t; R_{oj}, T_k)| - u)^2 dt}{A_i \int_{-\infty}^{+\infty} \hat{P}^2(t; R_{oj}, T_k) dt} \quad i = 1, 2, \dots, n \quad (17)$$

$$u \leq \hat{P}(t; R_{oj}, T_k)$$

given in equation (17). Here $\hat{P}(t; R_{oj}, T_k)$ is the deconvolved seismogram based on R_{oj} , T_k and u is an arbitrary but fixed level. A_i is the total time for which the magnitude of \hat{P} is greater than or equal to u . The lower integral represents the total energy in \hat{P} for $u = 0$. Figure 10 illustrates how C is determined. The $C(u; R_{oj}, T_k)$ function is defined for various amplitude levels u , and thus represents the energy of \hat{P} above the value u per unit time, i.e., the energy concentration above a given u .

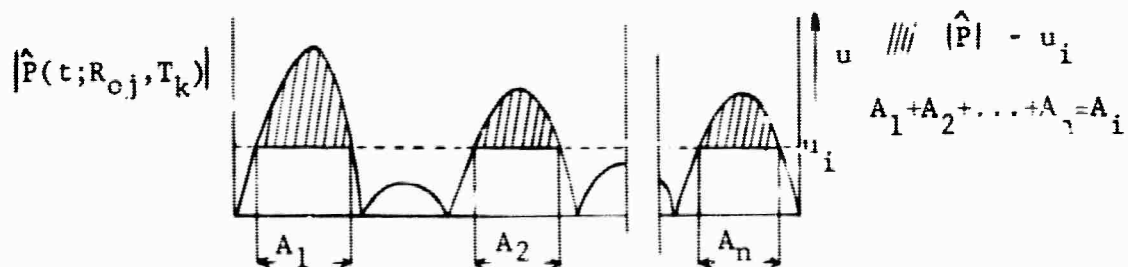


Fig. 10. Diagram of the parameters involved in the formulation of the simplicity criterion.

We choose as the correct estimate of $P(t)$, that $\hat{P}(t; R_{oj}, T_k)$ which maximizes $C(u; R_{oj}, T_k)$ for the smallest value of u . $C(u; R_{oj}, T_k)$ as a function of u will have a maximum for a single inverse filtered primary-ghost impulse pair when u just exceeds the magnitude of the largest secondary spike (for example the output $h^{-1}(t)*h(t)$ of Figure 7). Thus $C(u; R_{oj}, T_k)$ will decrease beyond this value of u . It will also be clear from Figure 9 that a maximum in concentration for $z(t)$ will occur for a larger value of u , and furthermore the maximum will not be as great as that for $z(t)$ in Figure 7. This is because the A_i in the denominator of $C(u; R_{oj}, T_k)$ for $z(t)$ in Figure 9 will be large compared to the A_i for $z(t)$ in Figure 7. Appendix A presents a proof that a choice of primaries based on this criterion is valid when the seismogram consists of a single impulse without noise, and the inverse filter procedure is exact.

Part of the object of this thesis is to test the validity of this same criterion when applied to more realistic data such as synthetic seismograms, and real earthquake records.

For earthquake seismograms, we visualize a choice of primaries made by the criterion discussed above as implying that the earth produces the minimum number of primary events. Thus the function $r(t)$ in equation (1) will be representative of an earth with the fewest number of major discontinuities as opposed to one with many minor boundaries. This implies that the most correct set of primaries relative to the other inverse filtered seismograms, will concentrate its energy in the fewest number of large pulses. Or in other words, it will be visually the simplest in structure. For this reason we refer to the criterion as the simplicity criterion.

It is useful for illustrative purposes to plot C as a function of delay time T when u is held constant. The value of T for which this function achieves a maximum when u is a minimum provides the estimate \hat{T} for the correct value of delay time. \hat{T} will be the value of T_k used to produce the estimated primaries, \hat{P} . In the next section we discuss how \hat{T} is converted into focal depth.

Conversion of \hat{T} into Focal Depth: The seismogram itself cannot give us a direct estimate of the focal depth. However, if the velocity structure in the area of the source is known and the value of \hat{T} is obtained from the seismogram, then the focal depth can be computed with travel-time equations. However, we cannot expect this velocity information to be available in the area of each seismic disturbance. Since this is the case, it is suggested that an average velocity structure could be constructed from known P-wave velocities as a function of depth. (Birch et al (1942) and Gutenberg (1955, 1958) have compiled this information). This average velocity profile may be mathematically approximated by a piecewise linear velocity function (Steinhart, 1961) of the form

$$V_{j+1} = V_j + b_j(Z_{j+1} - Z_j) \quad (18)$$

where V_j is the P-wave velocity at depth Z_j , b_j is the rate of change of velocity with depth, and the subscript "j" refers to the j^{th} second order velocity discontinuity in the downward direction. We can compute the time for a P-wave to travel from Z_j to Z_{j+1} using

$$t_j = \frac{1}{b_j} \left[\cosh^{-1} \left(\frac{1}{\sin \varphi_j} \right) - \cosh^{-1} \left(\frac{1}{\sin \varphi_{j+1}} \right) \right] \quad (19)$$

(Steinhart, 1961). Here φ_j is the angle of incidence of the P-wave path of travel with a discontinuity at depth Z_j . The horizontal distance traversed by the P-wave going from Z_j to Z_{j+1} is given by

$$x_j = \frac{V_j}{b_j \sin \varphi_j} (\cos \varphi_j - \cos \varphi_{j+1}). \quad (20)$$

The angle of incidence of P-waves with the earth's surface for various distances has been theoretically computed by Jeffreys and Bullen (1940). Nuttli and Whitmore (1961) made an observational determination of P-wave incidence angles. This information, combined with observed travel times for a zero focal depth P-wave (Jeffreys, 1940) and the equations (19) and (20) will enable us to construct travel-time curves for P and pP, for different focal depths. The procedure for doing this is as follows: First a depth of focus Z_j and an epicentral distance d are chosen. For this distance the angle of incidence of a P-wave is found. Then t_j and x_j are computed for the depth Z_j . To get the time of travel of the ghost (pP), t_j is added to the P-wave zero focal depth travel time (T_0) for the distance d . The epicentral distance for pP for the focal depth Z_j will be $d + x_j$. Now for the P-wave generated at this depth the reverse is true. The time t_j is subtracted from T_0 and its epicentral distance will be $d - x_j$. In a similar manner the remainder of the travel-time curve can be constructed for Z_j by varying d . The parameters involved are

illustrated in Figure 11.

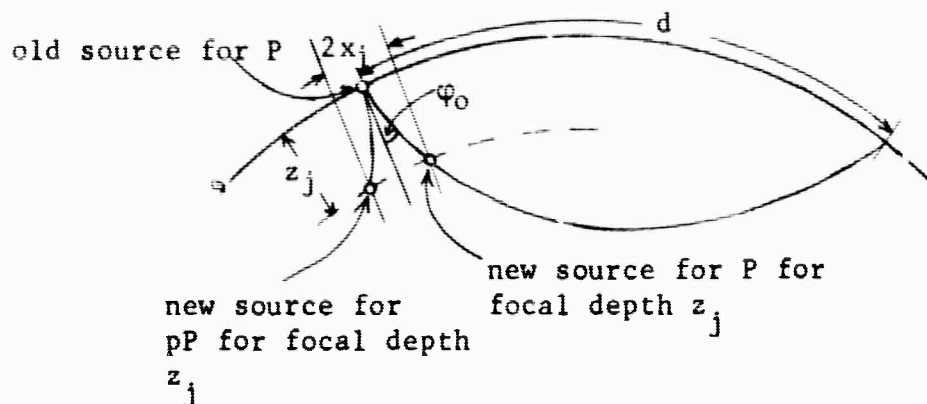


Fig. 11. Parameters involved in constructing travel-time curves for P and pP.

This completes the procedure to be evaluated in this thesis. It has three distinct advantages:

1. No estimate of earth filtering is required.
2. A direct estimation of T can be obtained.
3. Subjectivity by the user is minimized.

A disadvantage of the method is that the length of the inverse operator is directly proportional to the estimated focal depth. For large focal depths this requires operating on a longer portion of the input signal. This could result in storage problems in the computer and also increase the computation time quite rapidly.

Scope and Limitation of Study

This study systematically evaluates a method designed to estimate two parameters contained in a band-limited signal that obeys the

doublet hypothesis.

Synthetic data is used for all experimental evaluation. Earthquakes were analyzed to test both the procedure and the assumptions on "live" (actual) data.

Only the most simple ghosting filter is assumed. However, the technique presented can easily be modified to accommodate more complex ghosting situations, with a corresponding increase in computation.

II

PROCEDURE OF THE INVESTIGATION

Design of the Optimum Inverse Filters

Inverse filter arrays were generated using the computer for three noise to signal ratios (R) (low, medium and high noise level) and twelve ghost amplitudes (R_0) ranging from 0.1 to 1.2. Each operator contains twenty points. This number of points was chosen as a compromise between expense of running the computer and increased effectiveness of a long inverse operator. An inverse operator designed for a specific R and R_0 combination may be modified for any delay time T , simply by making the spacing between filter points equal to that of the desired delay time. This is true because the inverse filter is a sampled function (sampled at 0.1 second intervals) which is zero everywhere except at multiples of T (Foster et al, 1964). Appendix II contains diagrams of the filter arrays used in this thesis.

It is interesting to observe that the inverse operator designed for small ghost amplitudes consists essentially of one point and hence the convolution operation will simply return the original signal. The envelope of these inverse operators is another interesting feature. When the noise to signal power ratio is large the operator effectively reduces to two points, one positive and the other negative. Such an operator will do very little to estimate the primaries.

Both these features are to be expected, since for low amplitude ghosts very little filtering is required to suppress them. Also, when

signals are recorded with a high background noise level very little can be done to recover the primary signal.

Synthetic Signals

For the purposes of evaluating the effectiveness of the procedure, synthesized synthetic data containing three primary-ghost pairs were generated in the computer. Important signal parameters were built into the data. These included variable delay times, ghost amplitudes and random noise. The most important single parameter is the delay time, since the effectiveness of the procedure is based on its ability to estimate T for small primary ghost separations in the presence of noise and limited bandwidth of the signal.

A reasonable crustal model was assumed that would generate at least three primary-ghost pairs in a short interval of time. Figure 12a is a diagram of the crustal layering. It represents an average of several profiles given by Steinhart (1961). Three $r(t)$ functions were derived for focal depths of 2.5, 5.0 and 10.0 kilometers. The amplitudes of the primaries, were determined from amplitude versus angle of incidence curves based on Zoeppritz equations (Steinhart, 1961). Figure 12b illustrates the three $r(t)$ functions after convolution with $h(t)$. A "modified" Benioff Geneva-Type seismograph system impulse response $b(t)$ was used to synthesize seismograms by convolution with the $h(t)$ filtered $r(t)$ function. By "modified" we mean that the impulse response used in this thesis has been expanded and is given by $b(t/2)$ rather than $b(t)$. This results in shifting the spectrum of the synthetics towards lower frequencies; an attempt to simulate

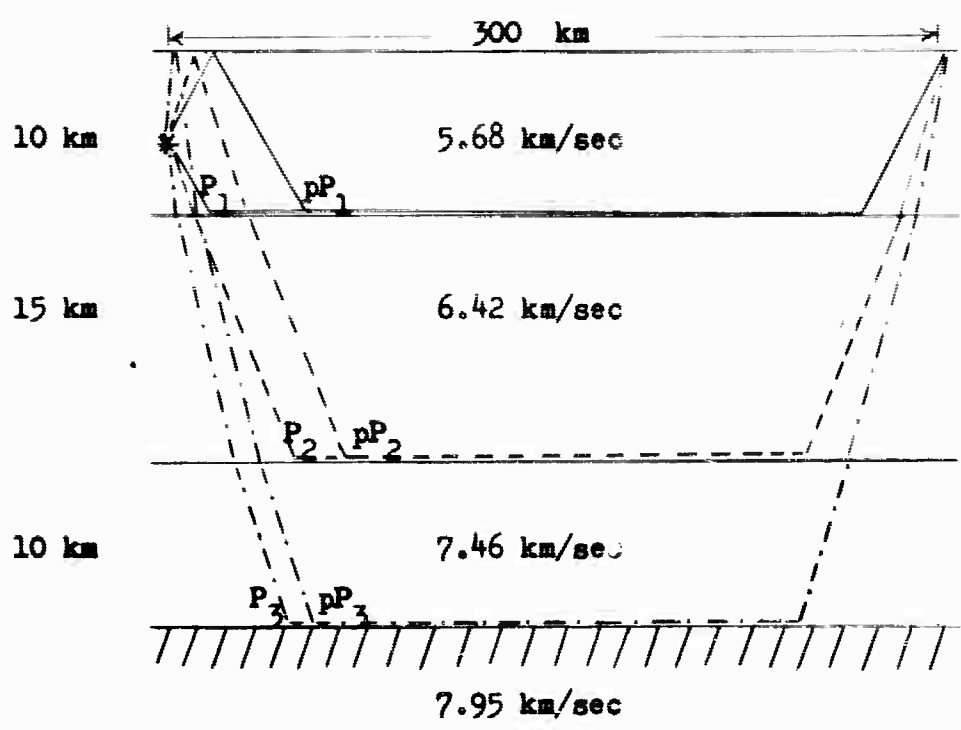


Fig. 12a. Crustal layering used to generate synthetic spikograms.

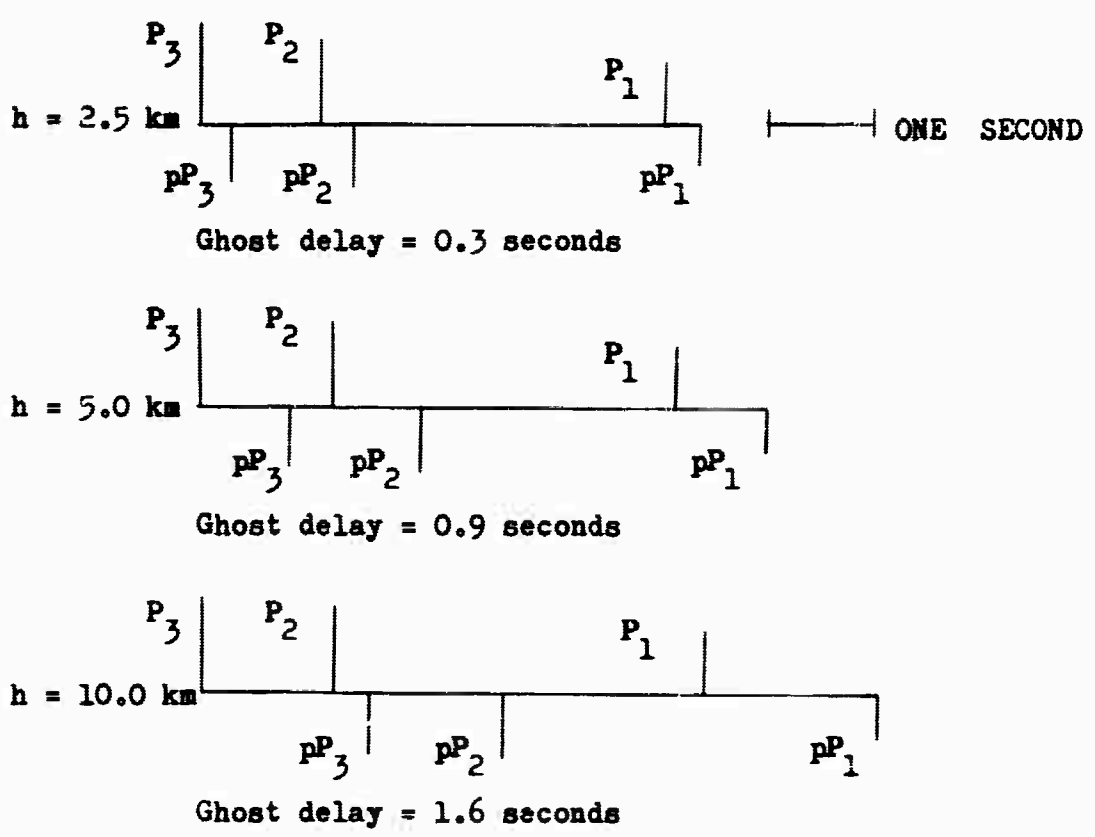


Fig. 12b. Synthetic spikograms for three focal depths.

attenuation in the earth. The impulse response curve and its frequency spectrum are illustrated in Figure 13. Random noise was generated in the computer with noise to signal power ratio equal to 0.01, 0.0625 and 0.25. These noises were then added to the filtered $r(t)$ function to produce the synthetic seismograms. The synthetic signals have the form

$$s(t) = b(t)*h(t)*r(t) + n(t).$$

By combining three groups of variables, T , R_0 and R in all possible independent combinations, twenty-seven different signals were generated. Table 1 lists the values for these parameters.

TABLE 1. Values for T , R_0 and R used to construct synthetic seismograms.

Focal depth in km	T (sec)	R_0	R
2.5	0.3	0.4	0.0100
5.0	0.9	0.7	0.0625
10.0	1.6	1.0	0.2500

Figure 14 is a block diagram of the evaluation procedure for synthetic signals. The first step is the selection of three inverse filters designed for the R built into the signal $s(t)$. Each one is designed for a different ghost amplitude. A range of delay times is chosen. Only one ghost amplitude and delay time combination is correct for $s(t)$. The signal is then convolved with each filter designed for

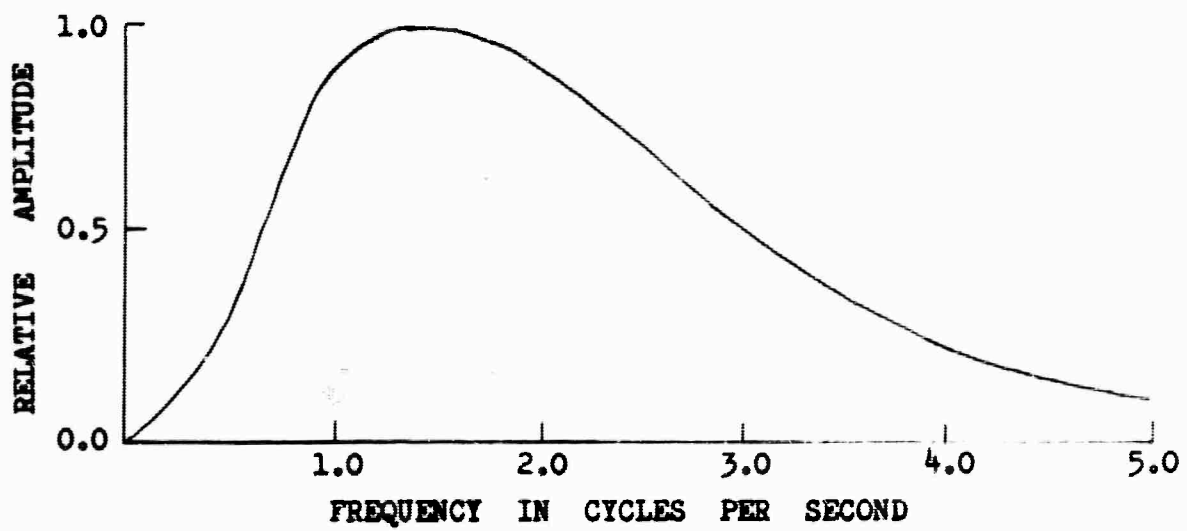
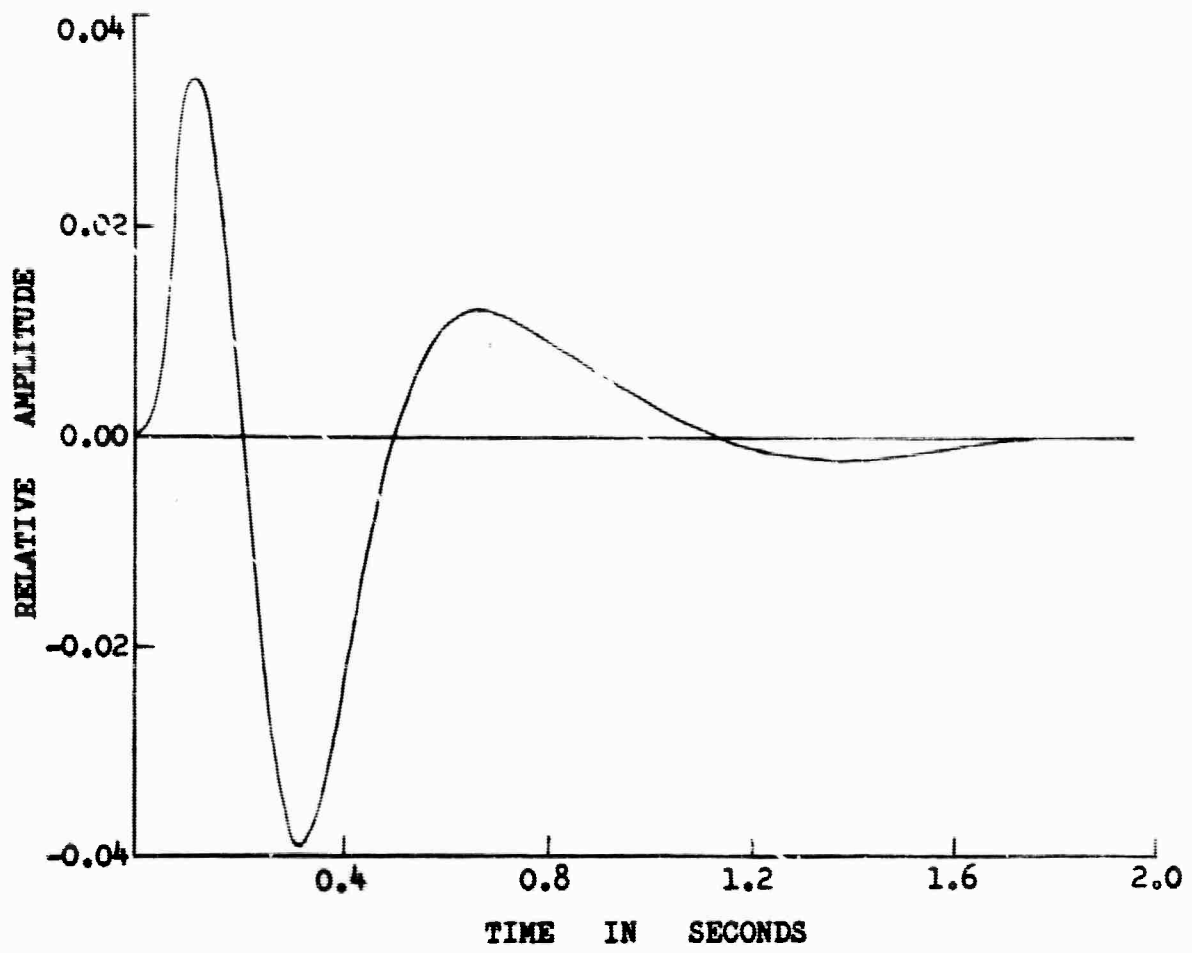


Fig. 13. Impulse and frequency response curves for the Benioff Geneva-type seismometer system.

1/2
AMES

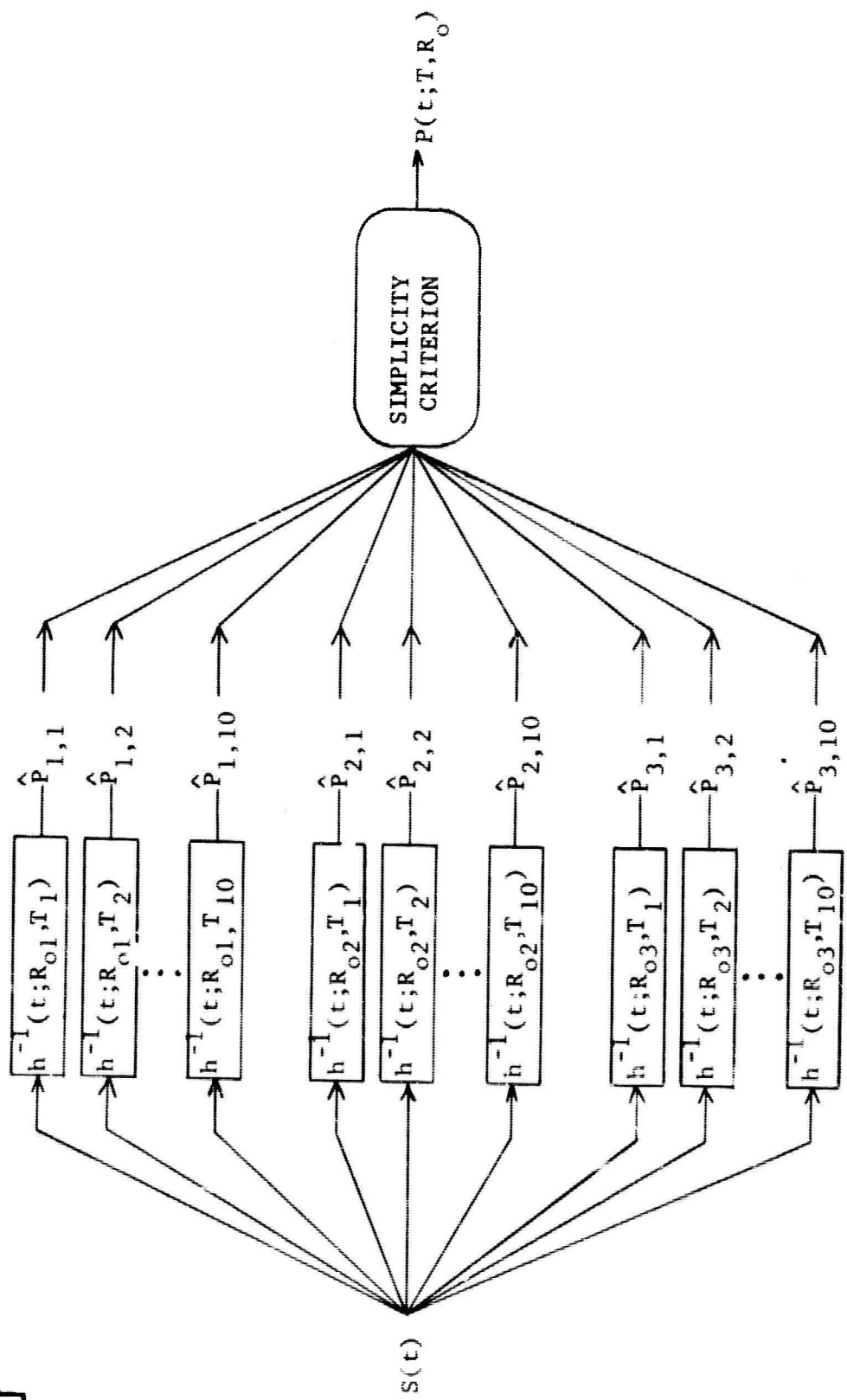


Fig. 14. Evaluation procedure for synthetic signals.

X

every delay time and ghost amplitude combination possible. This amounts to thirty separate convolutions. The simplicity of each output signal is measured for ten different u-levels (eg. 10 to 100% of maximum signal amplitude in 10% increments) using the simplicity criterion. The set of primaries $\hat{P}(t; \hat{R}_0, \hat{T})$ that most nearly satisfies the criterion is plotted together with $s(t)$ and the appropriate inverse filter. \hat{R}_0 and \hat{T} are the estimated parameters. If two or more output signals appear to satisfy the criterion equally well, then they are all plotted, so that they may be subjectively examined. This whole operation is performed on a computer. Appendix III describes the two main programs and several subroutines written to evaluate the delay time resolution for the procedure.

Earthquake seismograms were used to further evaluate the depth of focus estimation procedure. Theoretically determined delay times were converted into depths in order that they could be compared with published focal depths for the same earthquakes. Since very little published information is available for focal depths less than 33 kilometers, it was necessary to construct travel-time curves according to the procedure discussed on pages 24, 25, 26. The lack of published information for shallow focal depths further reflects the failure of visual recognition techniques to obtain delay times for reasons already discussed, such as overlap of pulses and high background noise level.

Construction of the Travel-Time Curves

A velocity structure for the crust and mantle was constructed from available data. This structure combined with travel-times for a

zero focal depth P-pulse obtained from the Jeffreys-Bullen Seismological Tables (1940) was used to calculate travel-times for P and pP. The calculations were performed by a computer for depths of focus ranging from 5 to 100 kilometers, and epicentral distances from 500 to 10,000 kilometers. One of the more useful plots of the travel-times may be seen in Figure 15. Here depth of focus is plotted as a function of the travel-time difference of P and pP for constant epicentral distances. It is readily apparent that the time difference is almost independent of distance for depths less than 20 kilometers. Further, it is apparent that the rate of change of delay time with epicentral distance decreases as a function of epicentral distance for constant focal depth. The results of this theoretical model agree quite well with available data from earthquakes with depths of focus greater than 50 kilometers.

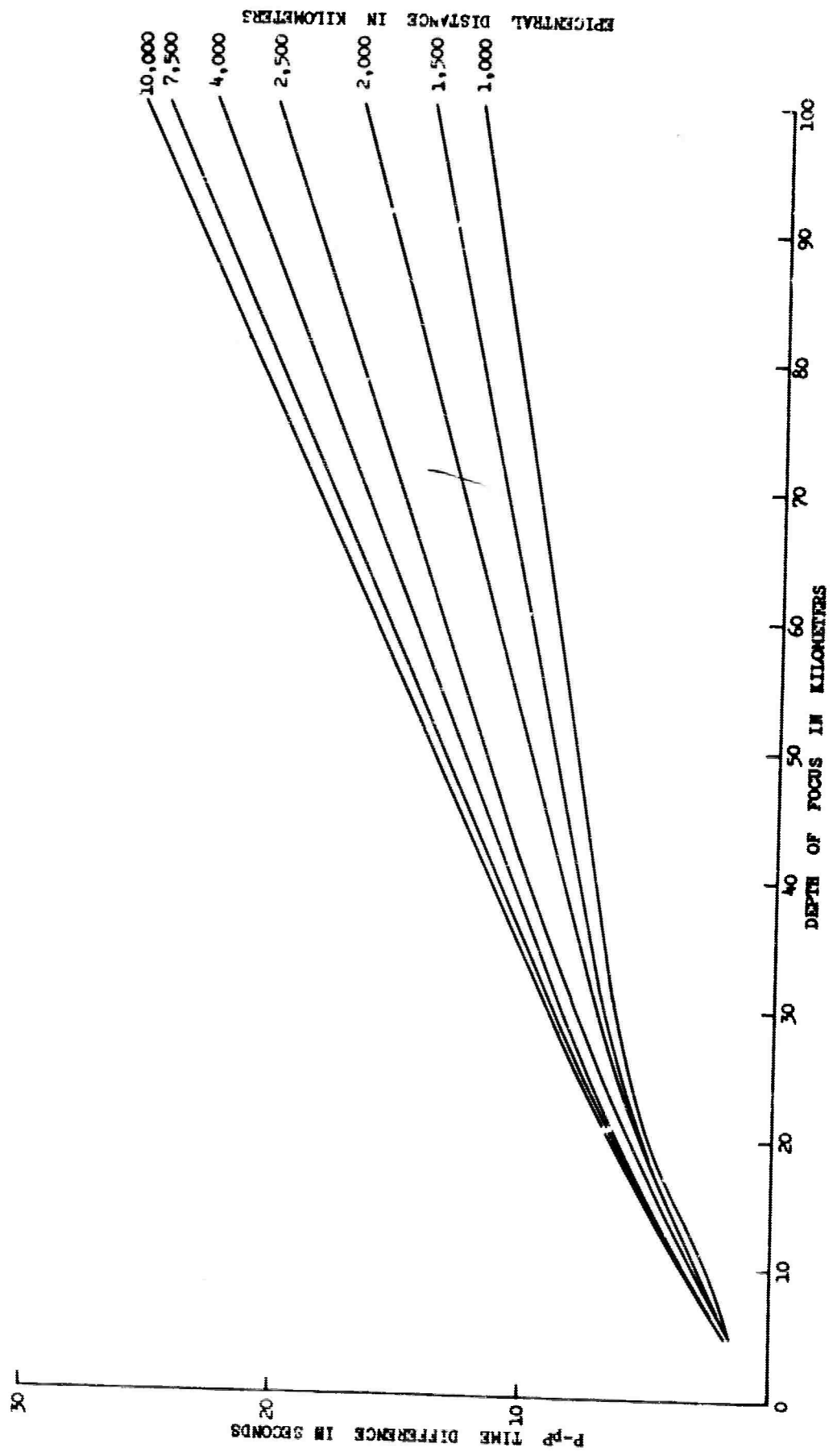


Fig. 15. Travel time curves for P-p time difference derived from a piecewise continuous velocity function.

Single Doublet Function

As an initial test the procedure was evaluated using a single doublet function (Figure 16 bottom diagram). The negative impulse was four tenths the amplitude of the positive spike. The delay time was half a second corresponding to four sample points in the function. Random noise at a level of 0.1 relative to the doublet was added.

For the analysis three inverse filters were designed for ghost amplitudes of 0.2, 0.4 and 0.6. The noise to signal power ratio used in the derivation of the inverse filters was 0.01. Delay times varied from 0.1 to 1.1 seconds in increments of 0.1 seconds. Each filter was modified for every delay time in the range and convolved with the doublet. The deconvolved signal was then measured for structural simplicity for ten different u -levels.

The results of this analysis are presented in Figures 16a through 16d. Figures 16a and 16b are plots of signal simplicity (energy concentration) as a function of delay time for specific u -levels. For $u = 0.1$ there is a definite high energy concentration corresponding to the filter designed for the correct delay time. The largest peak corresponds to the filter that was also designed for the correct ghost amplitude.

For the u -level 0.5 the magnitude of the peaks are considerably reduced. However, they do retain the same spacial orientation with

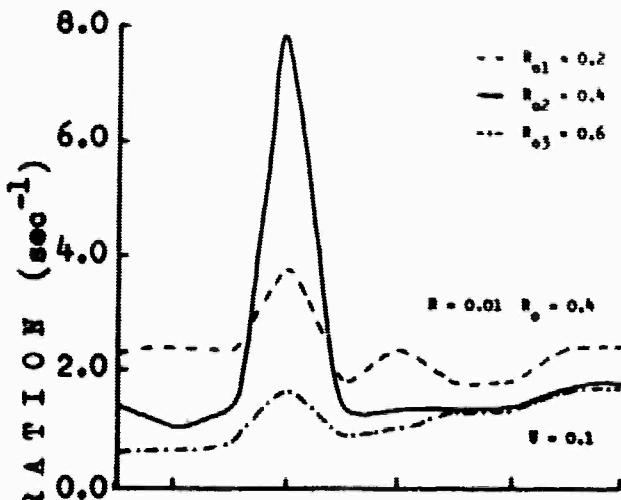


Fig. 16a. Energy concentration $C(T)$ versus delay time for $U = 0.1$.

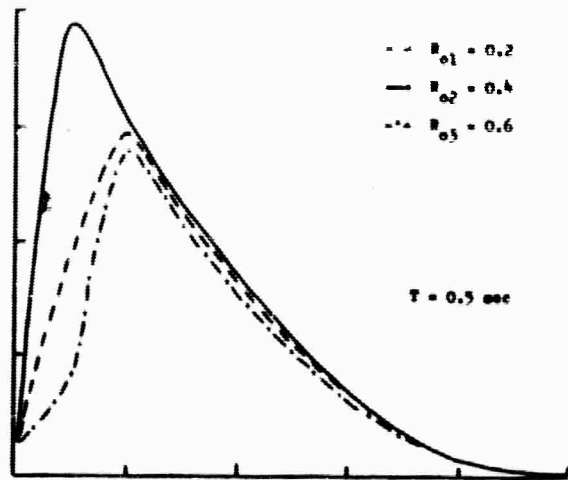


Fig. 16c. Energy concentration $C(U)$ versus u-level for $T = 0.5$ sec.

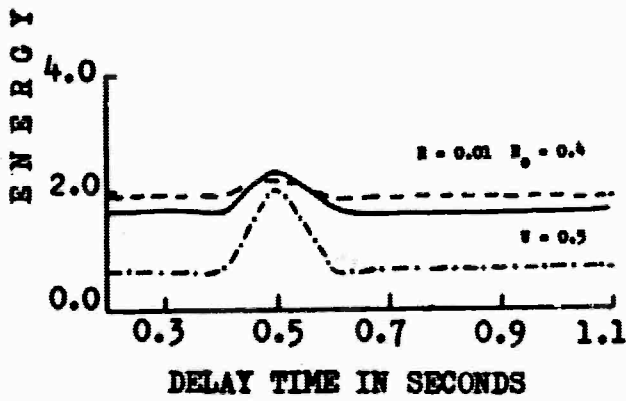


Fig. 16b. Energy concentration $C(T)$ versus delay time for $U = 0.5$.

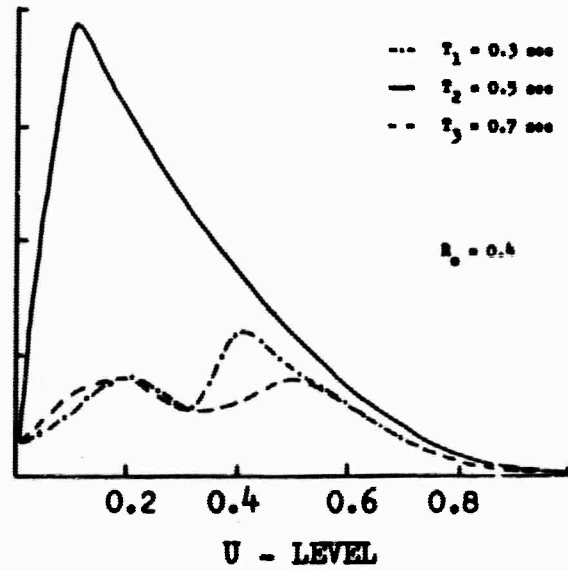


Fig. 16d. Energy concentration $C(U)$ versus u-level for $R_0 = 0.4$.

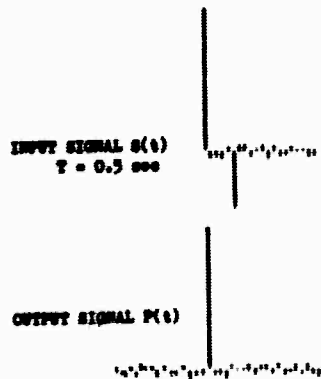


Fig. 16. Results of analysis of single doublet function.

respect to T. Both sets of curves indicate that our theoretical considerations are correct.

To further demonstrate the ability of the procedure for selecting the correct delay time and ghost amplitude, two more sets of energy concentration curves were constructed. Figure 16c is a plot of energy concentration for the correct delay time versus u-level. For small u-levels the curves are separated and indicate that the procedure produces a maximum for the correct ghost amplitude as expected. However, for higher u-levels the energy curves tend to become superimposed. This is not the case when we consider energy curves for filters designed for the correct ghost amplitude but wrong delay time. Figure 16d clearly illustrates this fact.

Based on this analysis it is concluded that, the procedure is able to select from an array of inverse filters that filter which is designed for the ghost amplitude and delay time built into the doublet function.

Bandlimited Single Doublet Functions

Synthesized doublet functions were constructed by convolving the same doublet with the modified Benioff impulse response illustrated in Figure 13. Three delay times were chosen so that the following conditions would occur. First, for a delay time of 2.1 seconds the primary pulse would be completely separated from its ghost reflection. Second, for a pulse separation of 0.9 seconds they would partially overlap. And third, for a pulse separation of 0.5 seconds overlap would occur to such a degree that individual pulses would be visually difficult to identify.

Each signal was tested in the same manner that the impulse doublet was analyzed. Figure 17 shows the results. For the signal with a primary-ghost delay time corresponding to 0.5 seconds, subsidiary maxima appear in the energy concentration versus delay time curve. However, the maximum corresponding to the correct delay time is the most pronounced. It should be noticed by comparison with Figures 16a and 16b that band-limiting does decrease the sensitivity (measured in terms of peak amplitudes) of the procedure.

Using the location of maxima as a guide, a filter was chosen which, convolved with the input signal, generated the best estimate of the primaries. The results of this operation for the three synthesized doublets is shown in the lower half of Figure 17. In all cases the original pulse shape has returned (compare with impulse response Figure 13), and the ghost has been effectively suppressed. Thus for these three cases the procedure has been successful in establishing which combination of R_{oj} and T_k was correct.

Bandlimited Triple Doublet Functions

Before testing the criterion on earthquake seismograms a sequence of synthetic signals was generated that contained three primary-ghost combinations. The construction of these signals is discussed in Part II (Synthetic signals). Three primary pulses were chosen to simulate actual earthquakes with shallow focal depths at small epicentral distances. Small epicentral distances were considered to be a greater challenge to the procedure for the same number of primary pulses, since proximity of primaries is more likely than for

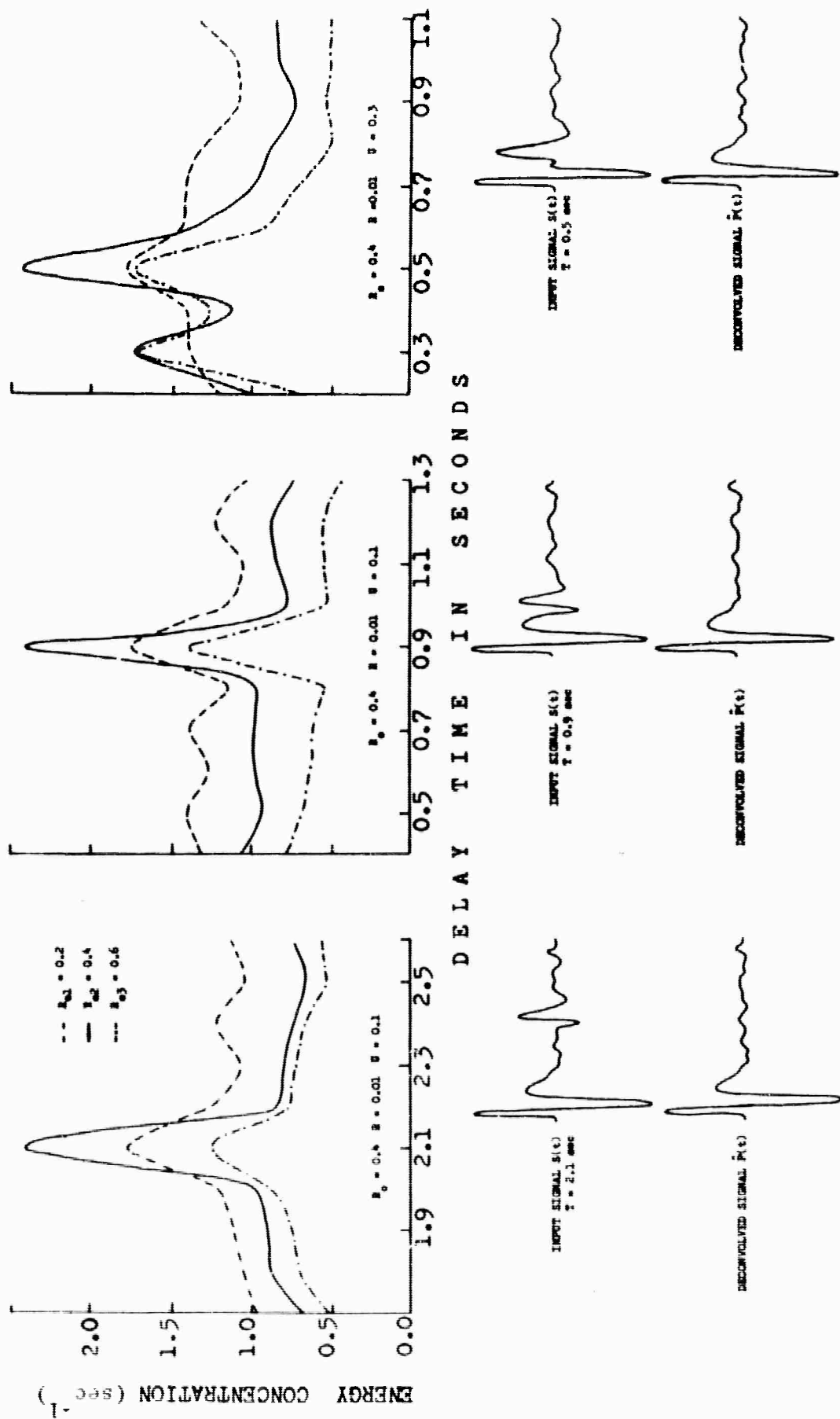


Fig. 17. Simplicity criterion used to determine the correct ghost delay time for three band-limited doublet functions containing random noise.

teleseismic (large) epicentral distances. For teleseismic distances, the procedure would yield essentially the same results as in the case of the single band-limited doublet, since the synthetic seismograms would essentially consist of a set of separated primary-ghost pairs.

Synthetic Signals for a 2.5 km Focal Depth: Nine synthetic signals for a delay time of 0.3 seconds were analyzed. Figure 18 illustrates these, together with the deghosted signals selected by the simplicity criterion (Figure 19). Several features in these figures are worth emphasizing.

With reference to Figure 18, synthetic signals for large ghost amplitudes ($R_o = 1.0$) are quite oscillatory. Individual pulse recognition is virtually impossible. In these cases the inverse operator designed for the correct ghost filter failed to improve the visual character of the synthetic signal.

The deghosted signal $\hat{P}(t)$ is in general broader-band than the input signal $S(t)$. Signals for $\hat{R}_o = 1.0$, $R = 0.01$ and $\hat{R}_o = 0.7$, $R = 0.25$ particularly emphasize this.

For $R_o = 0.7$, $R = 0.25$ and $R_o = 1.0$, $R = 0.625$ and $R = 0.25$, changing the design of the inverse operator did not substantially effect the energy concentration versus delay time curves. This indicates that the procedure seems to lose sensitivity as the ghost amplitude and noise to signal power ratio increase.

Except for $R_o = 1.0$, $R = 0.01$, the procedure selected the correct delay time built into these nine synthetic signals. For this exception a delay time of 0.2 seconds was chosen. This is only 0.1 second less than the correct delay time (0.3).

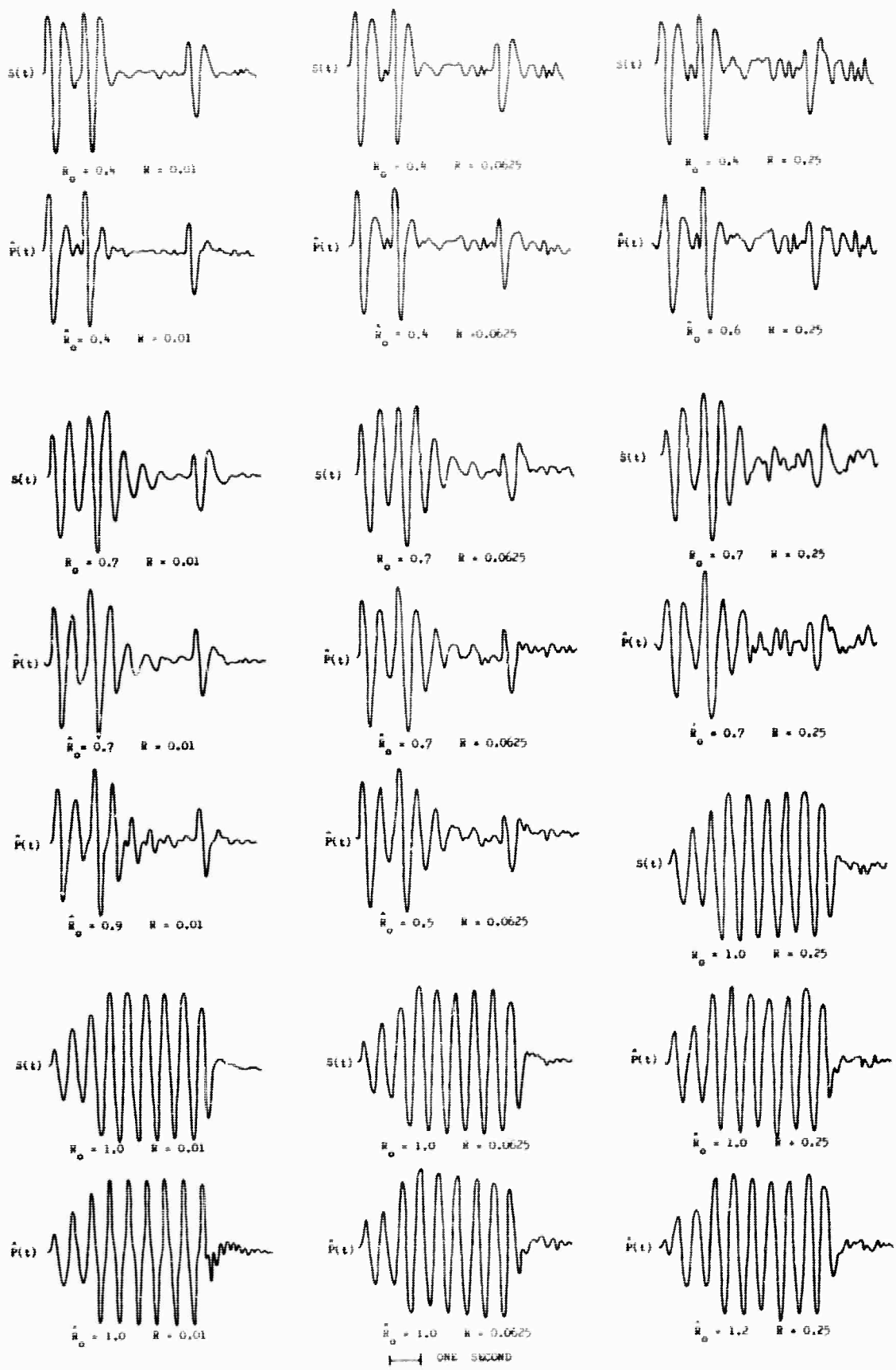


Fig. 18. Synthetic signals $S(t)$ for a 2.5 km focal depth (0.3 sec delay time) with their deghosted signals $\hat{P}(t)$ selected by the simplicity criterion.

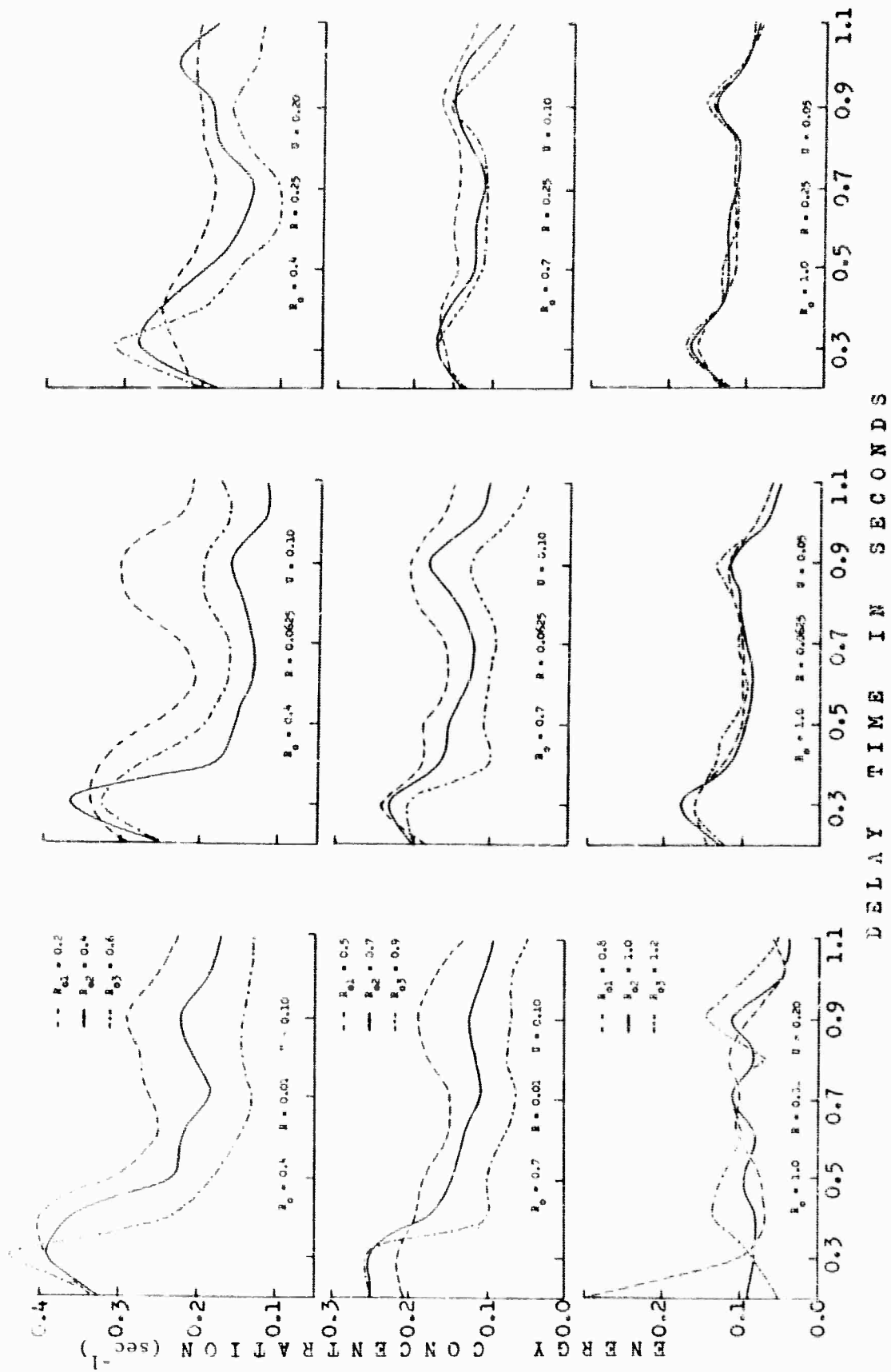


Fig. 19. Energy concentration $C(t)$ versus delay time for synthetic signals generated for a 2.5 km focal depth.

Synthetic Signals for a 5.0 km Focal Depth. Nine synthetic signals for a delay time corresponding to 0.9 seconds were analyzed. Figure 20 illustrates these together with the deghosted signals selected by the simplicity criterion.

Curves of energy concentration versus delay time for each signal are illustrated in Figure 21. For several cases these curves have two maxima, one at 0.3 seconds and the other at 0.9 seconds. The maximum at 0.3 seconds, although pronounced, is for an incorrect inverse filter which when convolved with the input signal fails to simplify it (in the sense defined in Primary-estimation Method). The cases where this is most obvious are $\hat{R}_0 = 0.6$, $R = 0.0625$ and $\hat{R}_0 = 0.5$, $R = 0.25$. For these cases the simplicity criterion was unable to differentiate the correct from the incorrect inverse filtered record. The reason for this seems to be that energy concentration increases with increasing bandwidth. Thus if an incorrect inverse filter overcompensates the spectrum of the input signal, as in the discussion on page 19, then the simplicity criterion may choose the incorrect version by virtue of its broader bandwidth over the correct version. This is a limitation of the procedure.

The procedure definitely helped to select the correct delay time in 5 out of the 9 synthetic signals analyzed. For $R_0 = 0.4$ and $R = 0.25$ the procedure selected 1.0 and 0.8 seconds for I . Either of these values differ only by 0.1 second from the correct value of I (0.9). For the three noise levels with $R_0 = 1.0$ the procedure was unable to estimate any delay time.

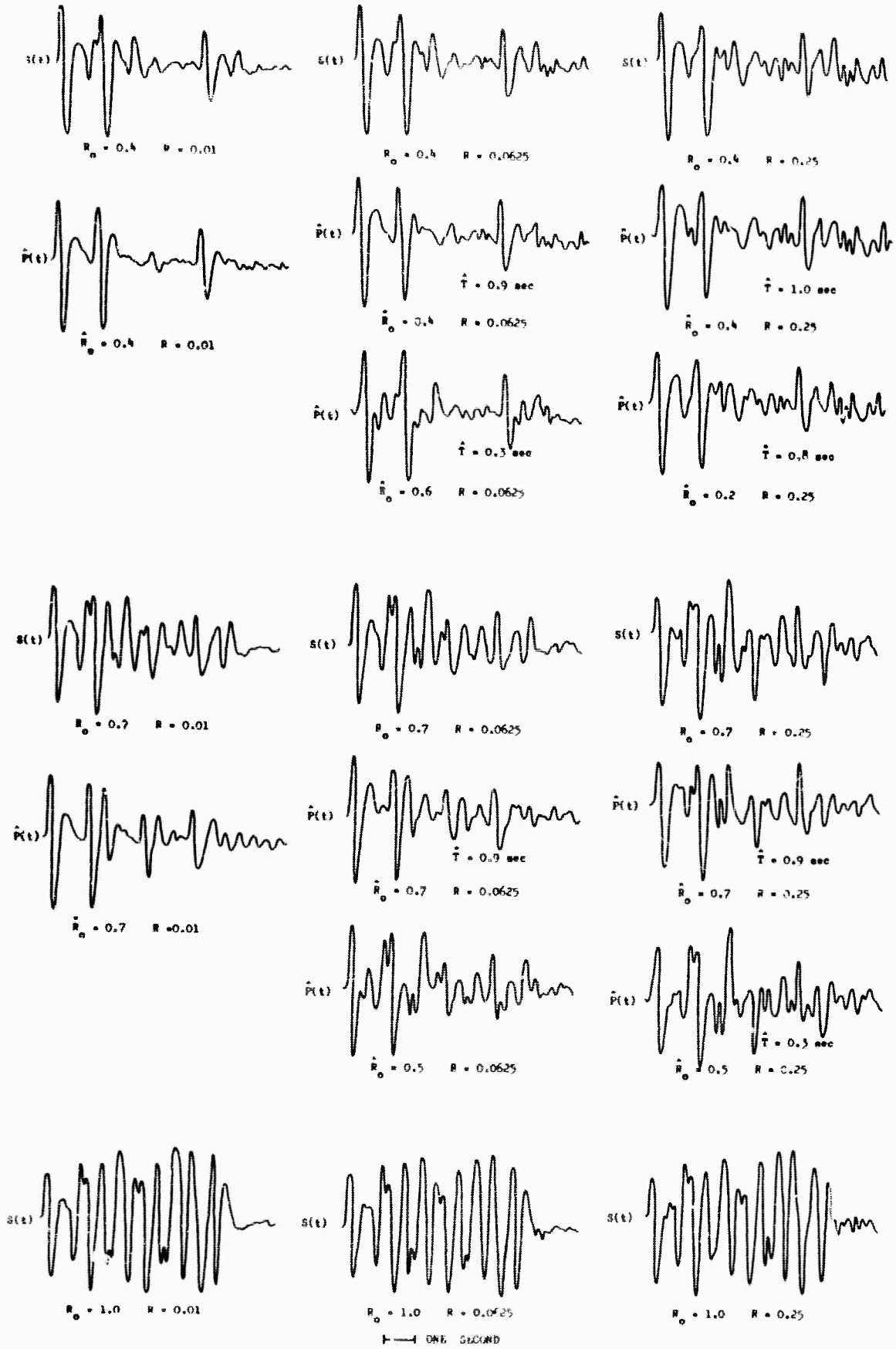
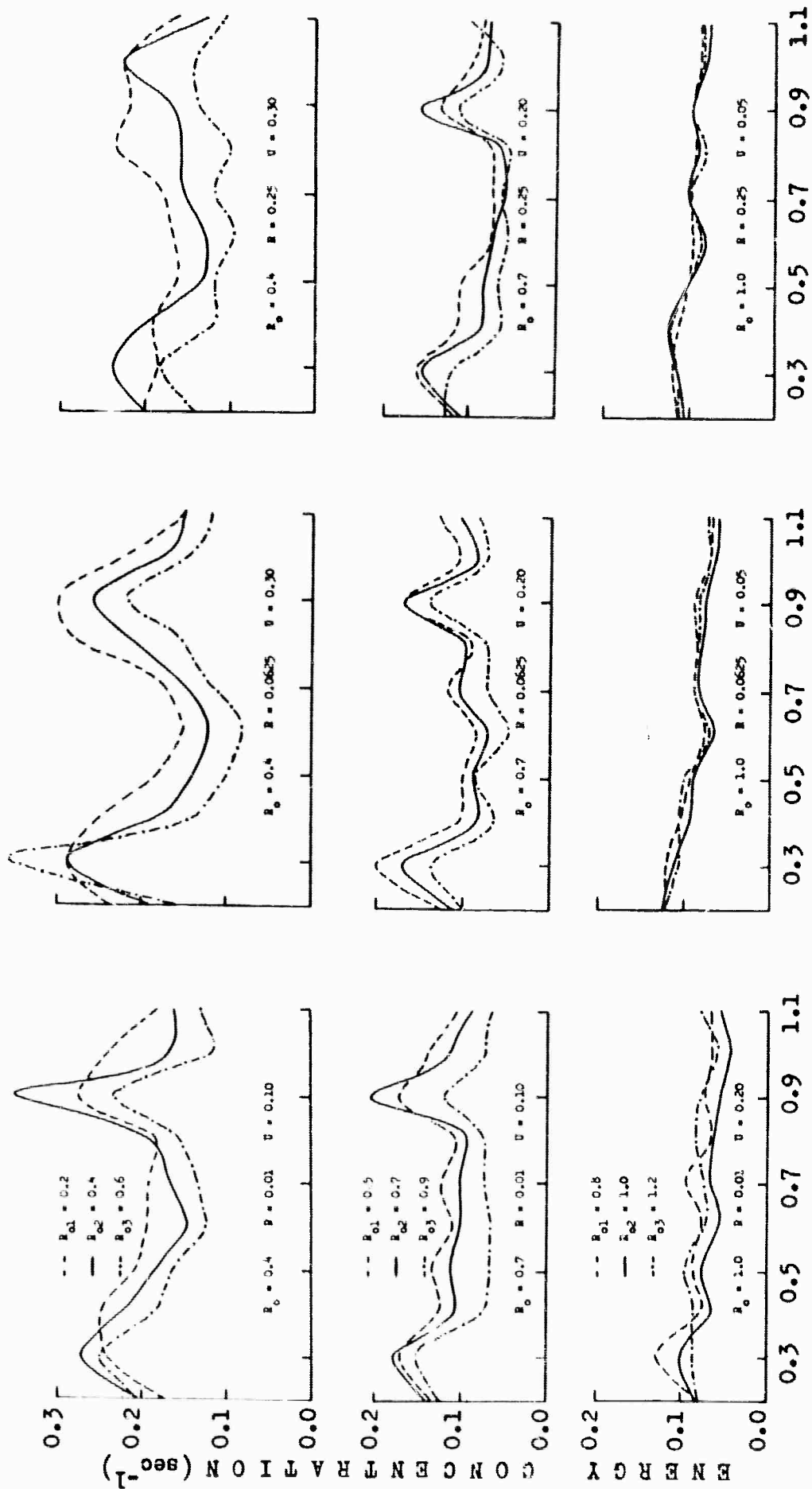


Fig. 20. Synthetic signals $S(t)$ for a 5.0 km focal depth (0.9 sec delay time) with their deghosted signals $\hat{P}(t)$ selected by the simplicity criterion.



DELAY TIME IN SECONDS

Fig. 21. Energy concentration (C(T)) versus delay time for synthetic signals generated for a 5.0 km focal depth.

Synthetic Signals for a 10.0 km Focal Depth: Nine synthetic signals for a delay time of 1.6 seconds were analyzed. Figure 22 illustrates these together with the deghosted signals selected by the simplicity criterion.

The set of energy concentration curves for this delay time are uniform in visual character (Figure 23). Only one maximum appears in each set of curves at a delay time of 1.6 seconds. These maxima give correct values for both T and R_0 in all cases, except for $R_0 = 0.4$, $R = 0.0625$; $R_0 = 0.4$, $R = 0.25$; and $R_0 = 1.0$, $R = 0.25$. For these three cases the procedure selected the correct delay time built into the synthetic signal, but not the correct R_0 .

The second ghost (third pulse) was not suppressed when the synthetic signal $S(t)$ contained ghosts with amplitudes greater than 0.7. Even though this may have been the case, the procedure was still able to select the correct delay time.

Analysis of Earthquake Seismograms

Four earthquake seismograms were chosen to test the estimation procedure on the basis of visual structure and the depth of focus as published by the USC&GS. Each earthquake was assumed to obey our mathematical model. A delay time and a ghost amplitude was found for each one using the procedure. The delay time was converted into focal depth using travel-time curves constructed from a piecewise continuous velocity function.

The deepest earthquake analyzed occurred in the Kurile Island region at a depth of approximately 60 kilometers. Its visual structure

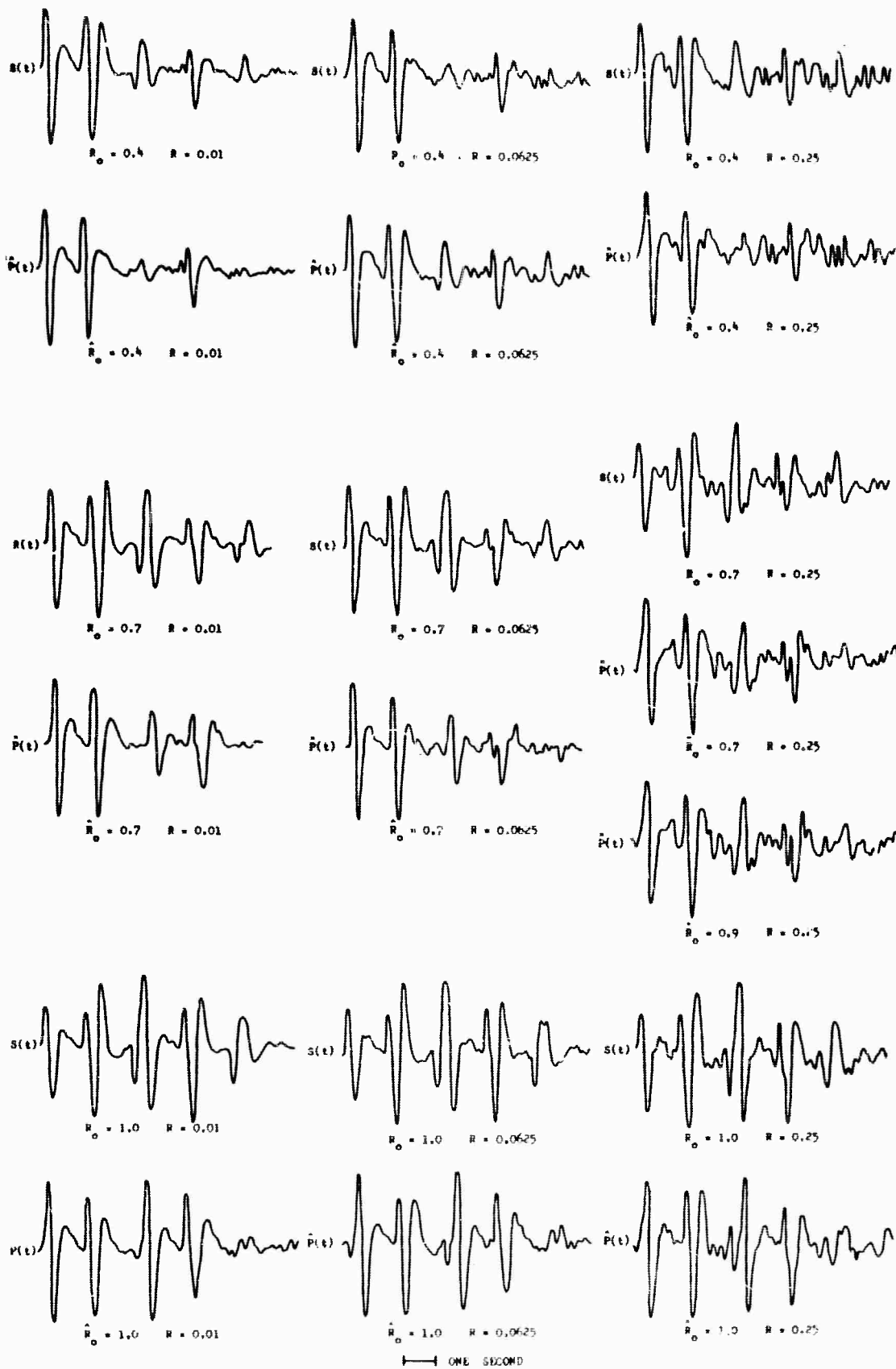


Fig. 22. Synthetic signals $S(t)$ for ~ 10.0 km focal depth (1.6 sec delay time) with their deghosted signals $\hat{P}(t)$ selected by the simplicity criterion.

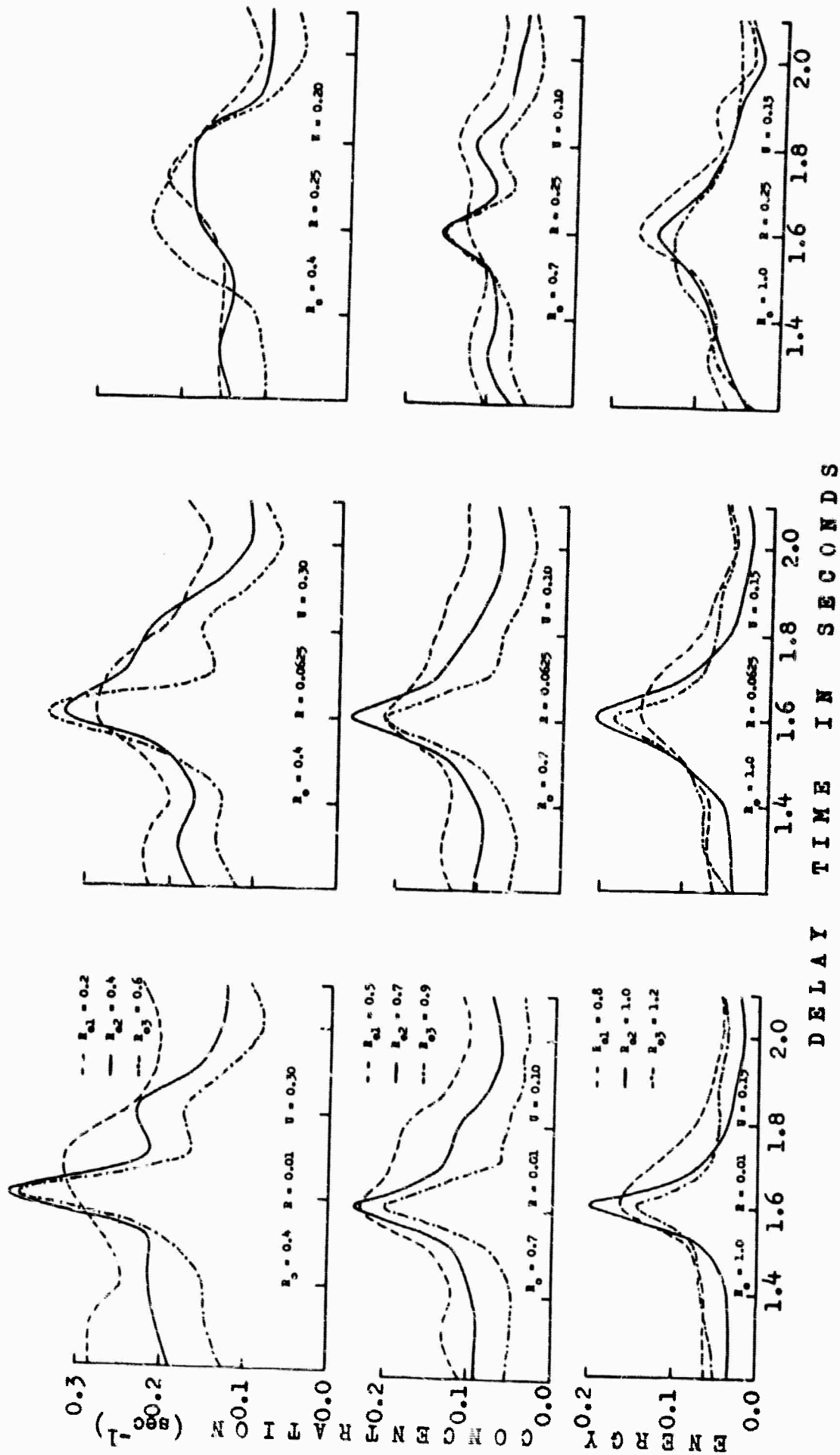


Fig. 23. Energy concentration (C(T)) versus delay time for synthetic signals generated for a 10.0 km focal depth.

is relatively uncomplicated (Figure 24 top). Apart from apparent noise only two large pulses are in the interval analyzed. A series of inverse operators were applied to the earthquake assuming a noise to signal power ratio of 0.25. This assumption appeared reasonable from visual inspection. Application of the procedure strongly indicated that the delay time is 12.7 seconds (Figure 25), which according to our travel-time curves corresponds to 45 kilometers. A ghost amplitude of 1.0 was estimated by the procedure. After applying the operator designed for these values a seismogram was obtained which is very similar to the input seismogram, except that the second pulse is completely suppressed. It should be noticed that the original pulse shape of the primary pulse has not been altered after deconvolution (Figure 24).

The second earthquake analyzed has a published focal depth of 44 kilometers. It occurred near Costa Rica almost 3500 kilometers from State College, Pennsylvania. An analysis of this signal produced two prominent peaks in the energy concentration versus delay time curve for a ghost amplitude of 0.8 (Figure 25). Two deconvolved seismograms were obtained using both the operators indicated to be most correct by the procedure. The operator designed for a delay time corresponding to 6.9 seconds has slighty suppressed the pulses following the primary, but has also boosted the apparent noise level. The second operator designed for a delay time of 8.7 seconds has successfully suppressed two pulses, but boosted the third pulse. This pulse has a shape almost identical in character to the first primary pulse. It appears too early in time to be associated with any known arrival for this earthquake. It has been suggested that if the 8.7 second operator is

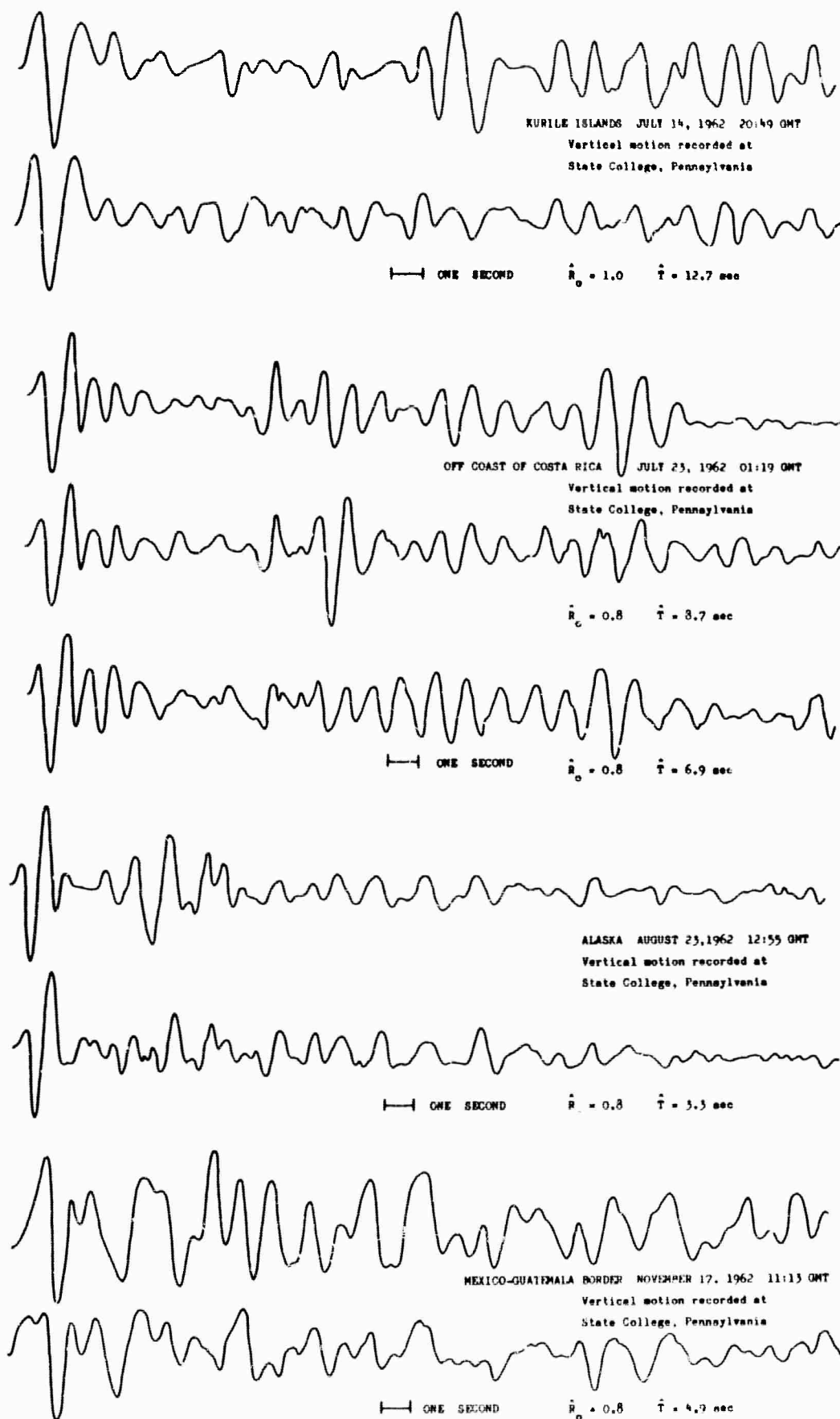


Fig. 24. Input earthquake seismograms and their deghosted counterpart selected by the simplicity criterion.

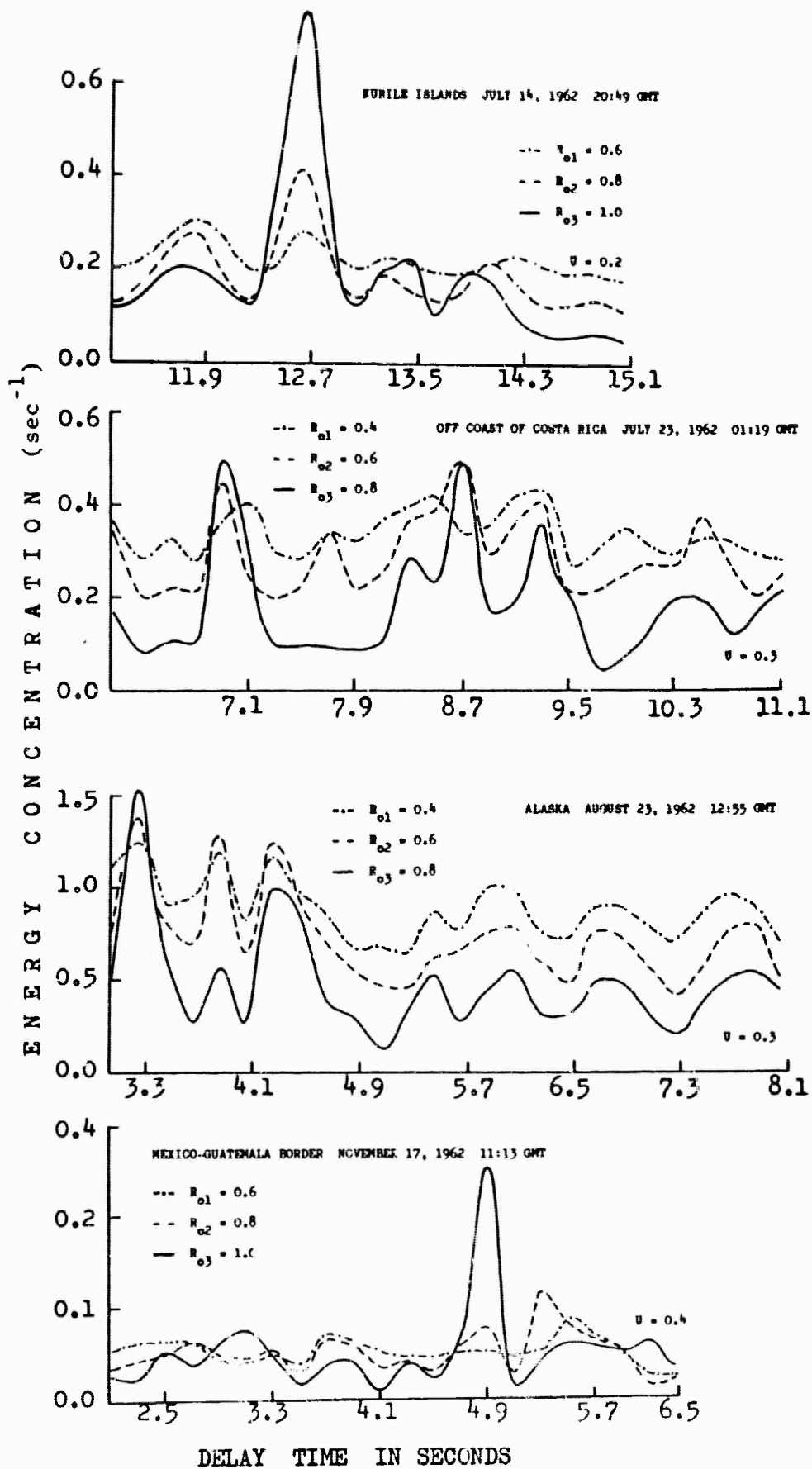


Fig. 25. Energy concentration ($C(T)$) versus delay time for earthquake seismograms.

correct, then this pulse is the first primary pulse from a second earthquake at the same source. Any conclusions in the matter drawn from a single earthquake seismogram represent only a judgement. It should be emphasized that the criterion cannot distinguish between the two operators from the information given. However, the fact that the apparent noise is boosted when the shorter operator is used makes one suspicious of this delay time. The longer delay time corresponds to a depth of focus of 31.5 kilometers.

Analysis of the third earthquake, whose source was in Alaska more than 5000 kilometers from State College, indicated that its depth of focus was 10 kilometers. Its published focal depth is 25 kilometers. This earthquake is relatively simple in structure with only two major pulses. The second pulse, if it is a ghost, is more oscillatory than the primary. The delay time for the maximum in the energy concentration curve was 3.3 seconds (Figure 24). Other maxima appear in the curve but the criterion dictates that the correct operator yields the greatest concentration of energy above the minimum value of u for the most likely delay time. This is the operator that should be chosen. The inverse filter corresponding to the 3.3 second delay time successfully suppressed the pulse following the primary. The rest of the signal remains relatively unchanged (Figure 24).

The last earthquake analyzed occurred at the Mexico-Guatemala border, and was computed by the USC&GS to have a 12 kilometer focal depth. The procedure estimated $\hat{T} = 4.9$ sec. and $\hat{R}_0 = 1.0$. $\hat{T} = 4.9$ sec. corresponds to a focal depth of 15 kilometers. This shallow earthquake seismogram has a visually complicated structure (Figure 24,

last earthquake pair). Individual pulses cannot be easily identified. However, the procedure very strongly suggests what R_0 and T should be. There is no ambiguity at all in this case (Figure 25). The deconvolved seismogram (Figure 24) is substantially simpler in structure compared to the original seismogram. Most of the pulses following the primary have been suppressed and no additional pulses have been created.

IV

SUMMARY AND CONCLUSIONS

This thesis is concerned with the problem of extracting information from a bandlimited signal in the presence of corrupting noise. In particular the signal is a seismic signal generated at or near the earth's surface. The information desired is a correct estimate of focal depth of the earthquake's source.

An accurate estimate of the source depth is a criterion that would help to differentiate between natural earthquakes and clandestine nuclear explosions.

Currently the USC&GS routinely publishes the focal depth of most earthquakes recorded on a world-wide basis. This depth, especially if the earthquake is shallow, may be in error by as much as 25 kilometers (Gunst and Engdahl, 1962).

Several investigators have suggested techniques that will give focal depth information. These techniques fall into three main categories: visual recognition procedures, spectral analyses and linear filter operations.

This thesis evaluates a technique for extracting delay time information from a signal that obeys a specific mathematical model. This model is assumed to be a reasonable approximation of the actual data generation process in the earth.

The method is based on the assumption that every seismic signal has passed through a ghost filter. This filter introduces a pulse

(ghost) after each primary pulse in the signal. It is delayed by a time that is related to the focal depth of the earthquake. Further, it is assumed that its polarity is reversed, but it retains the primary pulse shape. The ratio of the amplitude of the primary to its ghost is permitted to vary.

The estimation procedure uses optimum inverse filters of the doublet function (ghost filter) together with a criterion that measures the visual simplicity of a seismic signal convolved with an inverse filter. The inverse filters are designed to extract primary energy in the presence of ghost energy and random noise on the basis of a least-mean-square error criterion. Filter design is dependent on the delay time between primaries and ghosts, their amplitude ratio and noise to signal power ratio. The criterion was devised on the basis that a maximum in the energy concentration of the inverse filtered seismograms above a minimum level indicates which filter was most correctly designed. This is visualized as an expression of the assumption that the primary seismogram is generated by a few large discontinuities, rather than by many minor boundaries.

The technique was applied to bandlimited synthetic signals that contained several primary-ghost pairs in the presence of random noise. Each signal was convolved with an array of inverse operators, one of which was designed for the delay time, amplitude ratio and noise level built into the signal. The criterion was then applied to determine which operator was most correct. Of 27 synthetic signals which were analyzed, the procedure successfully selected the correct delay time in 22 cases. Figure 26 contains plots of the results of the analyses

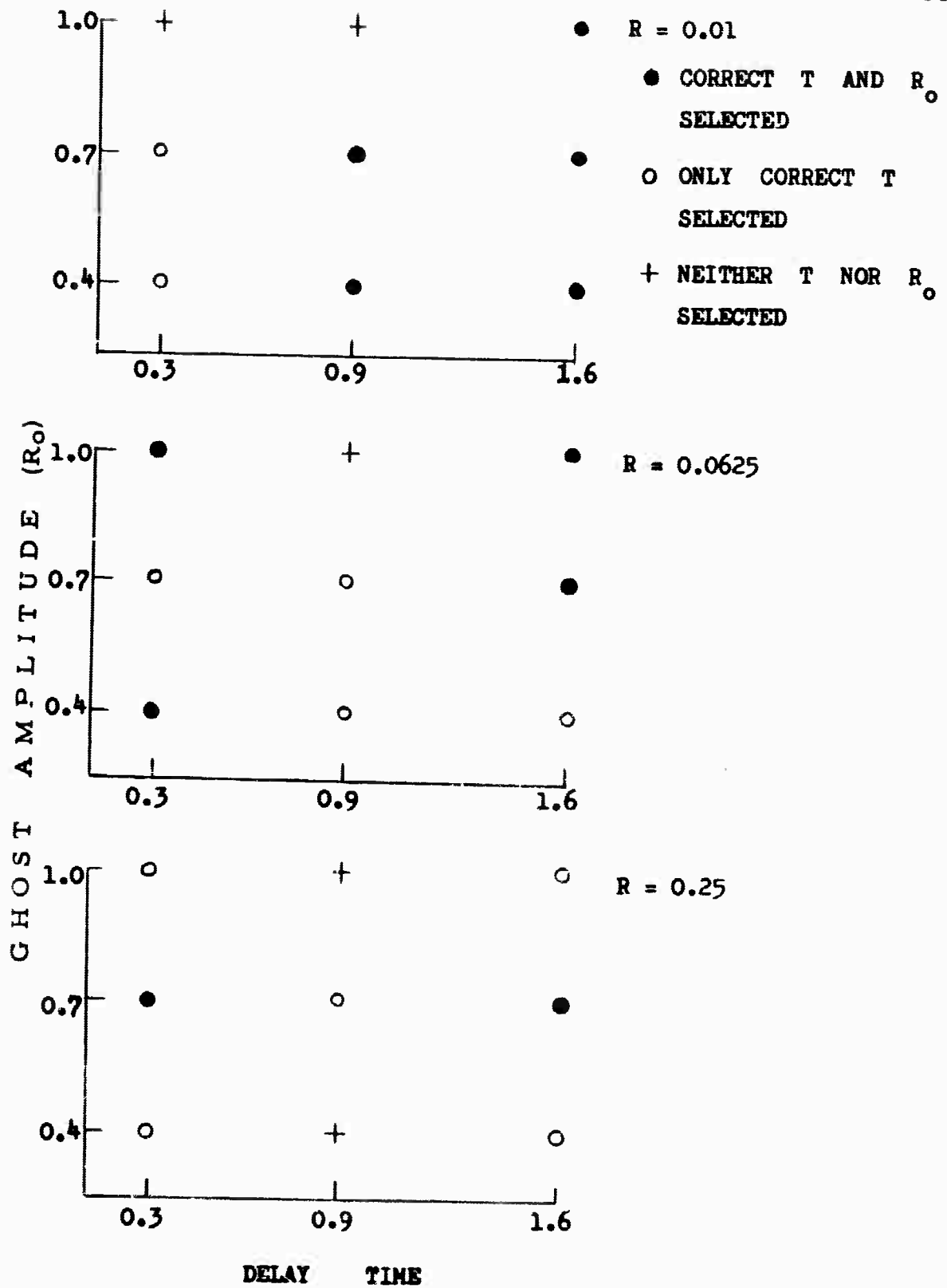


Fig. 26. Graphs summarizing the T, R_0 selection capability of the estimation procedure for the synthetic signals.

for three different noise to signal power ratios.

Four actual earthquake seismograms were then analyzed in the same manner. Focal depths computed from the selected delay times appeared quite reasonable when compared with depths for the same earthquakes published by the USC&GS. In all cases the inverse operator selected by the criterion considerably simplified the original signal.

On the basis of the results of the analyses of synthetic and earthquake signals it is concluded that the method has several distinct advantages. The three most important advantages are listed below.

1. No estimate of earth filtering is required.
2. A direct estimate of the delay time between primaries and ghosts is obtained.
3. Subjectivity by the user is minimized.

The following five statements summarize the effectiveness of the proposed focal depth estimation procedure.

1. Analysis of synthetic signals indicates that the sensitivity of the criterion decreases with increasing ghost amplitude, a decrease in bandwidth, and large noise to signal power ratio.
2. If more than one filter is predicted to be equally likely, then a visual examination of the deconvolved signals may be sufficient to determine which is correct.
3. The inverse filter selected by the criterion does simplify the visual character of the input signal.

4. The criterion in most cases is successful in choosing the correct inverse operator for band-limited synthetic signals of the type used.
5. Analysis of the earthquake seismograms indicates that the ghost filter assumption may be reasonable.

The method may be refined in several ways. First of all, the ghost filter may be made more complicated to account for additional pulses generated between the source and the earth's surface. The inverse operators could be made longer and hence more effective in reducing the doublet or ghosting function into a single impulse (Watson, 1964: personal communication). The criterion could be modified to remove its bias towards band-broadened signals. In this way some ambiguity might be removed and hence less subjectivity would be involved.

The estimation procedure certainly is encouraging enough to warrant further investigation. To establish fully the effectiveness of the procedure in accurately determining earthquake focal depths, several earthquakes recorded by many different stations should be analyzed. Consistency in the results obtained would also be a strong indication that the doublet hypothesis is a good assumption for earthquakes.

APPENDIX A. Proof of simplicity criterion for doublet function
with no noise and perfect inverse.

The criterion for a function $f(t)$ with sample values d_i may be written

$$C(u_i; R_{oj}, T_k) = \frac{\Delta t \left\{ \sum_{i=M_1}^{N_1} (|d_i \delta(t-i\Delta t) - u_i|^2) + \sum_{i=M_2}^{N_2} (|d_i \delta(t-i\Delta t) - u_i|^2) + \dots + \sum_{i=M_n}^{N_n} (|d_i \delta(t-i\Delta t) - u_i|^2) \right\}}{\Delta t \cdot A \sum_{i=1}^{NS} (d_i \delta(t-i\Delta t))^2 \Delta t}$$

Here the limits of the summations are functions of u and

$$(N_1 - M_1) + (N_2 - M_2) + \dots + (N_n - M_n) = A \leq NS,$$

where NS is the number of points necessary to specify $f(t)$ and Δt is the sampling interval of $f(t)$. Figure 27 illustrates the parameters involved in this analysis.

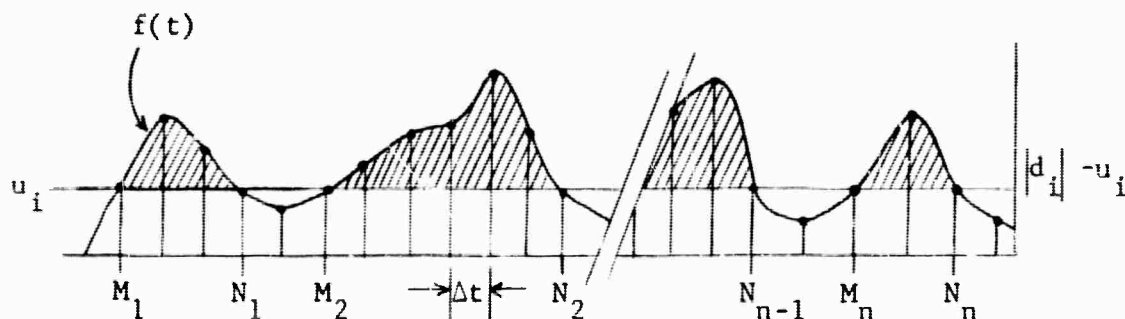


Fig. 27. Parameters involved in proof of simplicity criterion for doublet function with no noise and perfect inverse.

Let the result of deconvolutions with two inverse operators be a single impulse

$$f(t) = \begin{cases} d\delta(t-T_1) \\ 0 \end{cases} \quad t \neq T_1$$

and n impulses

$$f(t) = \begin{cases} d_1 \delta(t-T_1) \\ d_2 \delta(t-T_2) \\ \vdots \\ d_n \delta(t-T_n) \\ 0 \quad t \neq T_1, T_2, \dots, T_n. \end{cases}$$

For the single impulse $A = 1$ and

$$C(u_i; R_{oj}, T_k)_1 = \frac{[|d_1 \delta(t-T_1)| - u_i]^2}{1 \cdot \Delta t [d_1 \delta(t-T_1)]^2} \quad d_1 > u_i.$$

For n impulses $A = n$ and

$$C(u_i; R_{oj}, T_k)_n = \frac{[|d_1 \delta(t-T_1)| - u_i]^2 + [|d_2 \delta(t-T_2)| - u_i]^2 + \dots + [|d_n \delta(t-T_n)| - u_i]^2}{n \Delta t [d_1^2 \delta(t-T_1)^2 + d_2^2 \delta(t-T_2)^2 + \dots + d_n^2 \delta(t-T_n)^2]} \quad d_1, d_2, \dots, d_n > u_i.$$

Now for $u = 0$, $c(0; R_{oj}, T_k)_1 = \frac{1}{\Delta t}$ and $c(0; R_{oj}, T_k)_n = \frac{1}{n \Delta t}$.

Hence $c(0; R_{oj}, T_k)_1 > c(0; R_{oj}, T_k)_n$.

It is obvious that $c(0; R_{oj}, T_k)_1 > c(u_i; R_{oj}, T_k)_1$ for $u_i > 0$.

For the correct inverse operator $c(u_i; R_{oj}, T_k)$ will be a maximum for the smallest u -level. That is for a doublet function with no noise

the correct and ideal operator yields a single impulse as desired. Further, for this filter no other maxima will appear in the energy concentration versus u -level curve. However, maxima may appear in this curve for incorrect filters, but of course, not at the minimum u -level. This argument may be extended to more than one doublet with similar conclusions.

When noise is introduced into the system the minimum level for a maximum energy concentration is raised. The arguments of the proof, are similar to those outlined for the noiseless situation, except that an actual inverse filter is used.

APPENDIX B. Optimum inverse operators designed for the doublet function.

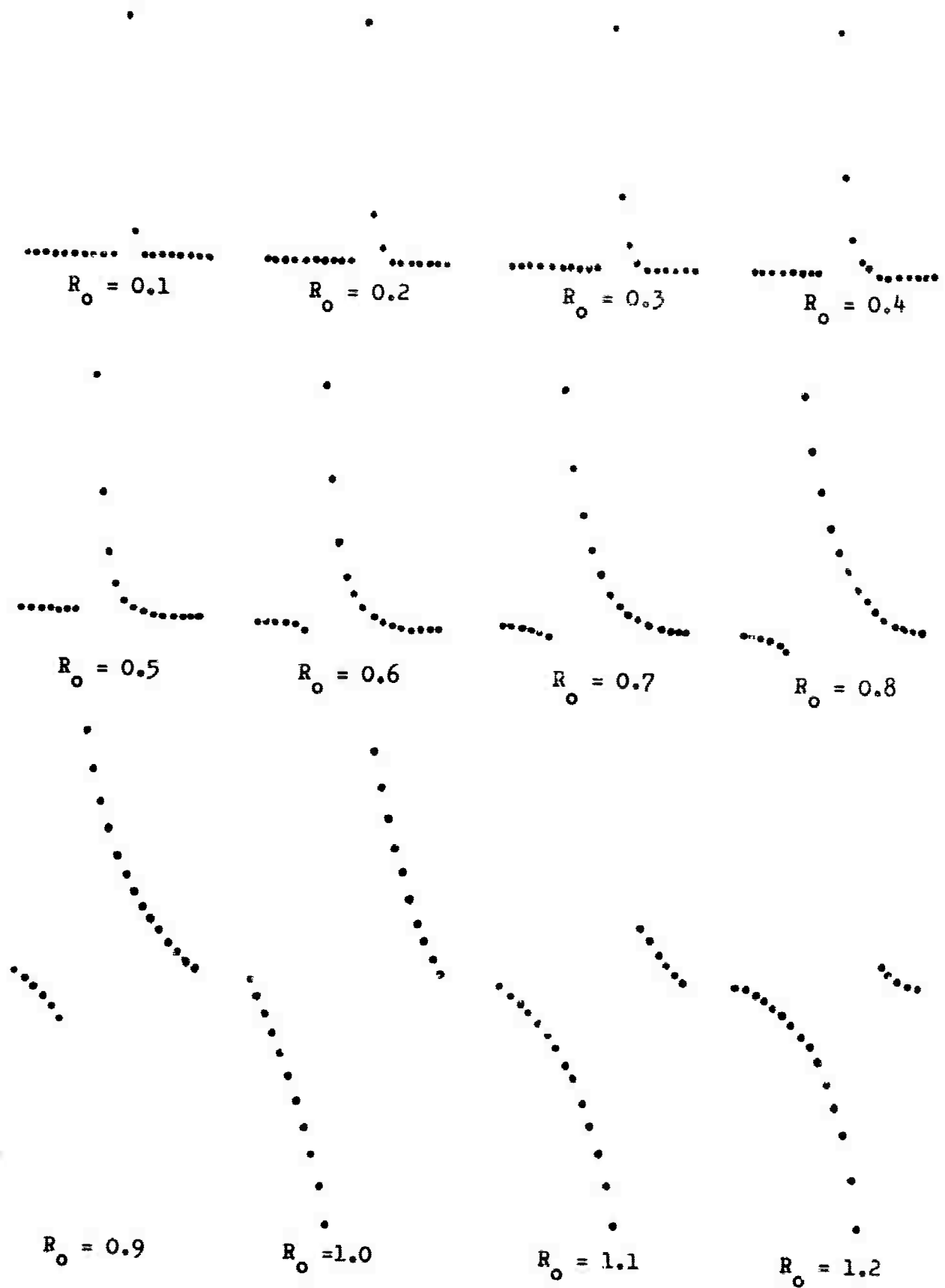


Fig. 28. Diagrams of twelve 20-point inverse operators designed for the doublet function for $R = 0.01$.

-0.0000	-0.0000	-0.0000	-0.0000	-0.0001	-0.0009
-0.0000	-0.0000	-0.0000	-0.0000	-0.0003	-0.0020
-0.0000	-0.0000	-0.0000	-0.0001	-0.0006	-0.0037
-0.0000	-0.0000	-0.0000	-0.0002	-0.0013	-0.0065
-0.0000	-0.0000	-0.0000	-0.0004	-0.0026	-0.0112
-0.0000	-0.0000	-0.0000	-0.0010	-0.0053	-0.0190
-0.0000	-0.0000	-0.0001	-0.0025	-0.0108	1.0000
-0.0000	-0.0001	-0.0003	-0.0065	1.0000	0.5877
-0.0001	-0.0004	-0.0012	1.0000	0.4918	0.3453
-0.0010	-0.0022	-0.0039	0.3946	0.2419	0.2029
1.0000	1.0000	1.0000	0.1557	0.1190	0.1193
0.0990	0.1979	0.2965	0.0614	0.0585	0.0701
0.0098	0.0391	0.0879	0.0242	0.0288	0.0412
0.0010	0.0077	0.0261	0.0096	0.0142	0.0242
0.0001	0.0015	0.0077	0.0038	0.0070	0.0142
0.0000	0.0003	0.0023	0.0015	0.0034	0.0083
0.0000	0.0001	0.0007	0.0006	0.0017	0.0048
0.0000	0.0000	0.0002	0.0002	0.0008	0.0028
0.0000	0.0000	0.0001	0.0001	0.0004	0.0015
0.0000	0.0000	0.0000	0.0000	0.0002	0.0007
$R_0=0.1$	$R_0=0.2$	$R_0=0.3$	$R_0=0.4$	$R_0=0.5$	$R_0=0.6$
-0.0311	-0.0029	-0.0093	-0.0734	-0.0317	-0.0146
-0.0632	-0.0062	-0.0192	-0.1482	-0.0644	-0.0299
-0.0973	-0.0105	-0.0305	-0.2260	-0.0989	-0.0469
-0.1344	-0.0164	-0.0439	-0.3083	-0.1362	-0.0663
-0.1757	-0.0246	-0.0604	-0.3968	-0.1777	-0.0894
-0.2225	-0.0366	-0.0812	-0.4932	-0.2243	-0.1172
1.0000	1.0000	1.0000	-0.5995	-0.2774	-0.1513
0.8357	0.6806	0.7671	-0.7177	-0.3387	-0.1936
0.6974	0.4632	0.5882	-0.8504	-0.4098	-0.2462
0.5810	0.3152	0.4509	-1.0000	-0.4929	-0.3120
0.4826	0.2145	0.3453	1.0000	-0.5903	-0.3946
0.3954	0.1459	0.2640	0.8504	-0.7050	-0.4984
0.3286	0.0992	0.2014	0.7177	-0.8402	-0.6289
0.2681	0.0674	0.1530	0.5995	-1.0000	-0.7932
0.2159	0.0456	0.1153	0.4932	0.2467	-1.0000
0.1705	0.0307	0.0858	0.3968	0.1955	0.1055
0.1304	0.0204	0.0624	0.3083	0.1499	0.0783
0.0944	0.0131	0.0433	0.2260	0.1089	0.0553
0.0614	0.0078	0.0273	0.1482	0.0708	0.0353
0.0302	0.0036	0.0132	0.0734	0.0349	0.0172
$R_0=0.7$	$R_0=0.8$	$R_0=0.9$	$R_0=1.0$	$R_0=1.1$	$R_0=1.2$

Table 2. Values for twelve 20-point inverse operators designed for $R = 0.01$.

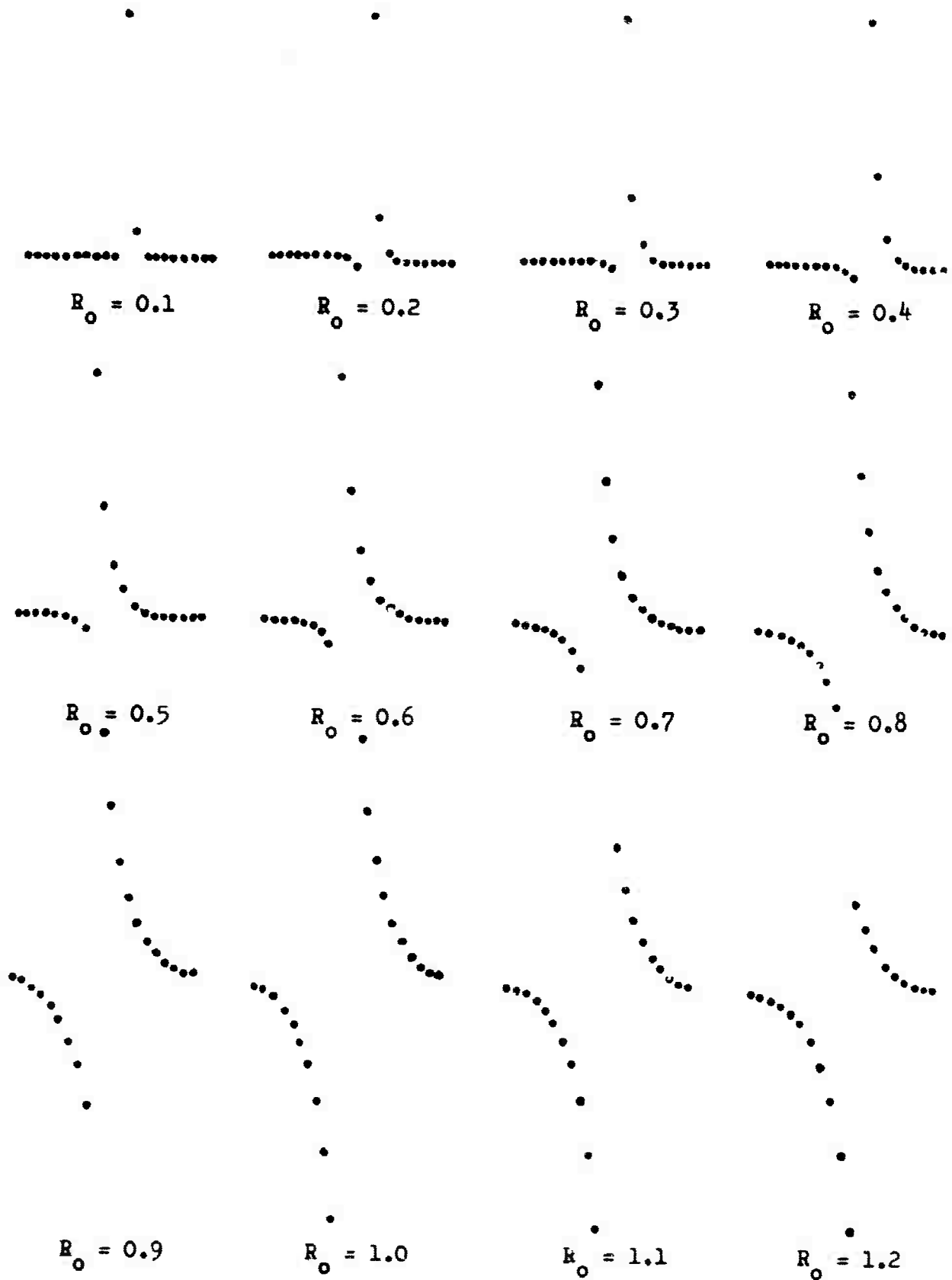


Fig. 29. Diagrams of twelve 20-point inverse operators designed for the doublet function for $R = 0.0625$.

-0.0000	-0.0000	-0.0000	-0.0000	-0.0002	-0.0009
-0.0000	-0.0000	-0.0000	-0.0000	-0.0005	-0.0021
-0.0000	-0.0000	-0.0000	-0.0000	-0.0011	-0.0041
-0.0000	-0.0000	-0.0000	-0.0001	-0.0025	-0.0079
-0.0000	-0.0000	-0.0000	-0.0003	-0.0056	-0.0148
-0.0000	-0.0000	-0.0001	-0.0007	-0.0122	-0.0279
-0.0000	-0.0001	-0.0005	-0.0018	-0.0270	-0.0523
-0.0001	-0.0005	-0.0018	-0.0050	-0.0594	-0.0980
-0.0006	-0.0025	-0.0063	-0.0136	1.0000	1.0000
-0.0060	-0.0131	-0.0227	-0.0368	0.4541	0.5333
1.0000	1.0000	1.0000	1.0000	0.2062	0.2844
0.0940	0.1873	0.2792	0.3687	0.0936	0.1517
0.0088	0.0351	0.0780	0.1359	0.0425	0.0809
0.0008	0.0066	0.0218	0.0501	0.0193	0.0431
0.0001	0.0012	0.0061	0.0185	0.0088	0.0230
0.0000	0.0002	0.0017	0.0068	0.0040	0.0123
0.0000	0.0000	0.0005	0.0025	0.0018	0.0065
0.0000	0.0000	0.0001	0.0009	0.0008	0.0034
0.0000	0.0000	0.0000	0.0003	0.0004	0.0017
0.0000	0.0000	0.0000	0.0001	0.0001	0.0007
$R_0=0.1$	$R_0=0.2$	$R_0=0.3$	$R_0=0.4$	$R_0=0.5$	$R_0=0.6$
-0.0031	-0.0060	-0.0151	-0.0213	-0.0135	-0.0103
-0.0070	-0.0130	-0.0323	-0.0453	-0.0288	-0.0222
-0.0127	-0.0223	-0.0540	-0.0750	-0.0479	-0.0377
-0.0218	-0.0357	-0.0830	-0.1140	-0.0735	-0.0592
-0.0366	-0.0554	-0.1234	-0.1673	-0.1091	-0.0902
-0.0609	-0.0849	-0.1806	-0.2415	-0.1593	-0.1356
-0.1012	-0.1296	-0.2626	-0.3459	-0.2310	-0.2029
-0.1680	-0.1973	-0.3805	-0.4935	-0.3337	-0.3026
1.0000	-0.3002	-0.5505	-0.7028	-0.4815	-0.4509
0.6029	1.0000	1.0000	-1.0000	-0.6940	-0.6716
0.3634	0.6576	0.6920	1.0000	-1.0000	-1.0000
0.2191	0.4324	0.4787	0.7028	0.5817	0.3669
0.1321	0.2842	0.3309	0.4935	0.4032	0.2462
0.0796	0.1866	0.2284	0.3459	0.2791	0.1651
0.0479	0.1223	0.1571	0.2415	0.1925	0.1104
0.0288	0.0797	0.1073	0.1673	0.1318	0.0734
0.0171	0.0514	0.0722	0.1140	0.0889	0.0481
0.0100	0.0322	0.0470	0.0750	0.0579	0.0306
0.0055	0.0187	0.0281	0.0453	0.0348	0.0180
0.0024	0.0086	0.0132	0.0213	0.0163	0.0084
$R_0=0.7$	$R_0=0.8$	$R_0=0.9$	$R_0=1.0$	$R_0=1.1$	$R_0=1.2$

Table 3. Values for twelve 20-point inverse operators designed for $R = 0.0625$.

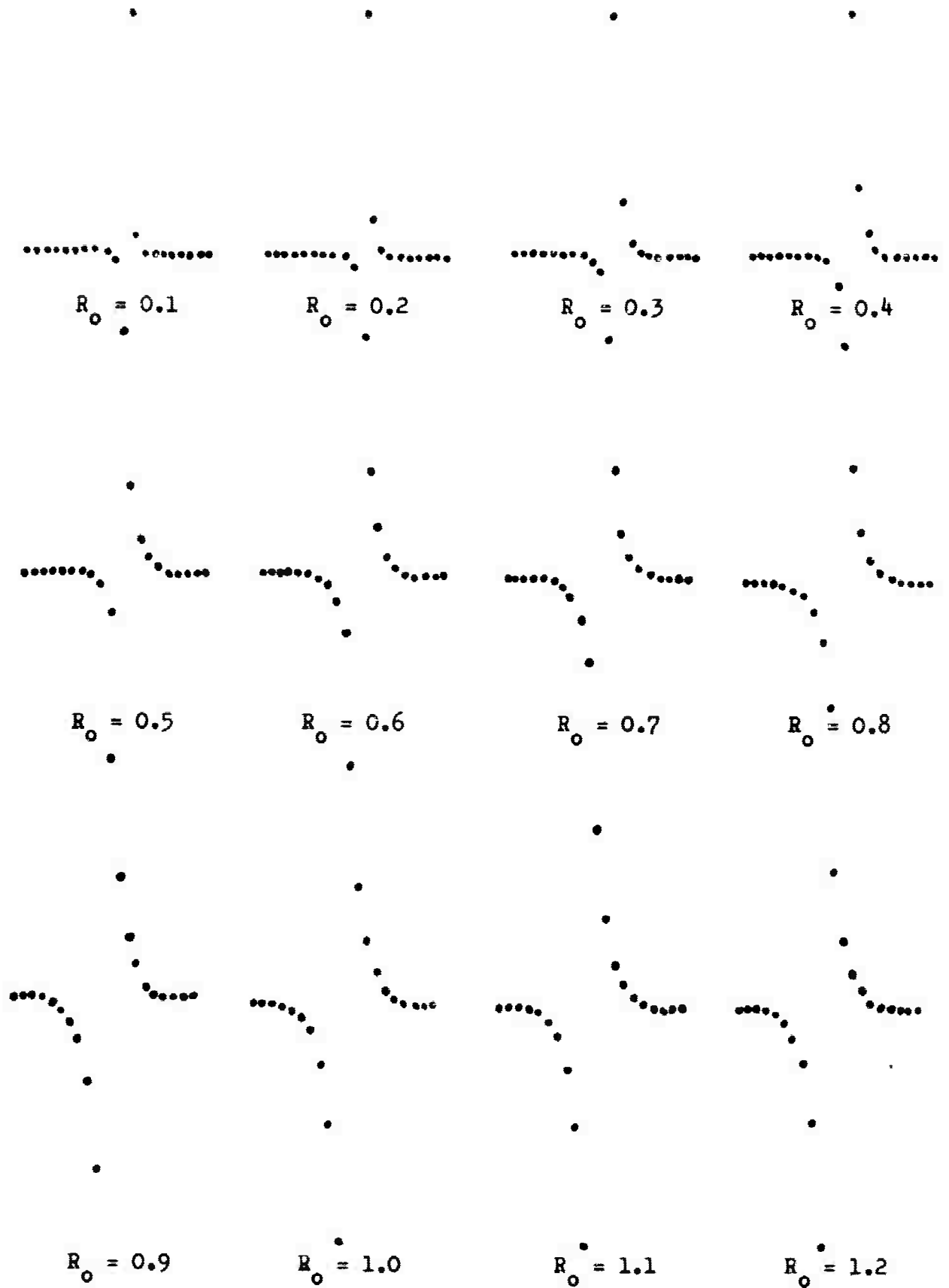


Fig. 30. Diagrams of twelve 20-point inverse operators designed for the doublet function for $R = 0.25$.

-0.0000	-0.0000	-0.0000	-0.0000	-0.0000	-0.0001
-0.0000	-0.0000	-0.0000	-0.0000	-0.0000	-0.0002
-0.0000	-0.0000	-0.0000	-0.0000	-0.0001	-0.0005
-0.0000	-0.0000	-0.0000	-0.0001	-0.0004	-0.0012
-0.0000	-0.0000	-0.0000	-0.0003	-0.0010	-0.0030
-0.0000	-0.0000	-0.0002	-0.0009	-0.0029	-0.0072
-0.0000	-0.0002	-0.0009	-0.0031	-0.0080	-0.0175
-0.0001	-0.0011	-0.0039	-0.0102	-0.0221	-0.0424
-0.0016	-0.0069	-0.0169	-0.0339	-0.0610	-0.1026
-0.0205	-0.0437	-0.0730	-0.1127	-0.1686	-0.2484
1.0000	1.0000	1.0000	1.0000	1.0000	1.0000
0.0797	0.1577	0.2320	0.3008	0.3619	0.4132
0.0064	0.0249	0.0538	0.0905	0.1310	0.1707
0.0005	0.0039	0.0125	0.0272	0.0474	0.0705
0.0000	0.0006	0.0029	0.0082	0.0172	0.0291
0.0000	0.0001	0.0007	0.0025	0.0062	0.0120
0.0000	0.0000	0.0002	0.0007	0.0022	0.0050
0.0000	0.0000	0.0000	0.0002	0.0008	0.0020
0.0000	0.0000	0.0000	0.0001	0.0003	0.0008
0.0000	0.0000	0.0000	0.0000	0.0001	0.0003
$R_o=0.1$	$R_o=0.2$	$R_o=0.3$	$R_o=0.4$	$R_o=0.5$	$R_o=0.6$
-0.0002	-0.0005	-0.0010	-0.0015	-0.0014	-0.0012
-0.0006	-0.0014	-0.0025	-0.0037	-0.0035	-0.0030
-0.0014	-0.0030	-0.0053	-0.0077	-0.0073	-0.0064
-0.0031	-0.0064	-0.0108	-0.0156	-0.0149	-0.0132
-0.0069	-0.0133	-0.0218	-0.0312	-0.0301	-0.0273
-0.0152	-0.0276	-0.0440	-0.0625	-0.0606	-0.0561
-0.0336	-0.0575	-0.0888	-0.1250	-0.1222	-0.1152
-0.0742	-0.1198	-0.1792	-0.2500	-0.2463	-0.2368
-0.1639	-0.2494	-0.3617	-0.5000	-0.4962	-0.4866
-0.3618	-0.5192	-0.7301	-1.0000	-1.0000	-1.0000
1.0000	1.0000	1.0000	1.0000	0.7522	0.5832
0.4529	0.4802	0.4954	0.5000	0.3733	0.2838
0.2052	0.2306	0.2454	0.2500	0.1852	0.1381
0.0929	0.1108	0.1216	0.1250	0.0919	0.0672
0.0421	0.0532	0.0602	0.0625	0.0456	0.0327
0.0191	0.0255	0.0298	0.0312	0.0226	0.0159
0.0086	0.0122	0.0147	0.0156	0.0112	0.0077
0.0039	0.0058	0.0072	0.0077	0.0055	0.0037
0.0017	0.0027	0.0034	0.0037	0.0026	0.0017
0.0006	0.0010	0.0014	0.0015	0.0010	0.0007
$R_o=0.7$	$R_o=0.8$	$R_o=0.9$	$R_o=1.0$	$R_o=1.1$	$R_o=1.2$

Table 4. Values for twelve 20-point inverse operators designed for $R = 0.25$.

APPENDIX C. Fortran computer programs.

Two main programs and several subroutines were written to perform the routine computations necessary to accomplish this thesis. They are written for the Pennsylvania State University IBM 7074 computer.

This appendix briefly describes the purpose of each program and how they may be used.

A. Identification

Title: Executive Program MINIMAX

Programmer: Merdler

Date: February 1964

B. Purpose

Coordinates the functions of several subroutines that compute the simplicity of a deconvolved signal.

C. Usage

1. Calling Sequence: None. This is a main program.

2. Space required: Approximately 4000 locations.

3. Input and Output Formats

a) Input

R	noise to signal power ratio
DELT	input signal sampling increment
KUT	total number of different delay times used
XNL	u-level increment
NU	total number of u-levels

Format (F10.5, F5.3, I5, F5.3, I5)

NF	number of sample points in inverse operator
RH	ghost amplitude (negative floating point number)
LAGF	inverse filter lag

Format (I5, F5.3, I5)

LAGS	del.	ime
------	------	-----

Format (I5)

b) Output

Printer

TEK	signal energy concentration for a particular u-level, LAGS, RH and R.
ULEV	u-level
RH	ghost amplitude
Z	delay time in seconds
LAGS	delay time in zeroes

Format (6X, E16.8, 5X, F5.3, 6X, F7.3, 5X, F6.3, 5X, I5)

```

PROGRAM MINIMAX FOR SYNTHETIC SIGNALS
INPUT GENERATES SIGNAL S(I)
CONVOL DEGHOSTS S(I) BY CONVOLUTION WITH F(I)
INVERSE FILTER OF DOUBLET FUNCTION
MINMAX DETERMINES BEST OUTPUT SIGNAL
USING SIMPLICITY CRITERION
DIMENSION F(50),S(500),U(100),F(100),T(100),RAND(500),G(1000),
1 BLIM(50)
READ 200,R,DELT,KUT,XNL,NU
CALL INPUT(S,NS,RH,LAGS)
PRINT 100
1 READ 220,NF,RH,LAGS
IF(NF)999,999,2
2 READ 230,(F(I)),I=1,NF)
DO 30 J=1,KUT
SUMJ=0.0
DO 20 I=1,NU
E(I)=0.0
20 T(I)=0.0
READ 240,LAGS
Z=FLOATF(LAGS+1)*DELT
CALL CONVOL(F,S,NF,NS,LAGS,XNL,NU,F,T,U,SUMJ)
DO 30 K=1,NU
IF(T(K))4,4,3
3 TEK=F(K)/(T(K)*DELT*SUMJ)
GO TO 5
4 TEK=0.0
5 ULEV=U(K)
30 PRINT 150,TEK,ULEV,RH,Z,LAGS
GO TO 1
100 FORMAT(1H1,12X,7HMINIMAX,8X,5HLEVEL,8X,5HG-AMP,6X,5HG-LAG,4X,6HZER
1 OES//)
150 FORMAT(6X,E16.8,5X,F5.3,6X,F7.3,5X,F6.3,5X,I5)
200 FORMAT(F10.5,F5.3,I5,F5.3,I5)
220 FORMAT(I5,F5.3,I5)
230 FORMAT(4E16.8)
240 FORMAT(I5)
999 STOP
END

```

```
PROGRAM SIMPTST FOR EARTHQUAKES
CONVOL DEGHOSTS S(I) BY CONVOLUTION WITH F(I)
INVERSE FILTER OF DOUBLET FUNCTION
MINMAX DETERMINES BEST OUTPUT SIGNAL
USING SIMPLICITY CRITERION
DIMENSION F(50),S(500),U(100),F(100),T(100)
READ 200,R,DELT,KUT,XNL,NU
CALL INPUT(S,NS,PH,LAGG)
PRINT 100
1 READ 220,NF,PH,LAGF
IF(NF)999,999,2
2 READ 230,(F(I),I=1,NF)
DO 30 J=1,KUT
SUM1=0.0
DO 20 I=1,NU
E(I)=0.0
20 T(I)=0.0
READ 240,LAGS
Z=FLOATF(LAGS+1)*DELT
CALL CONVOL(F,S,NF,NS,LAGS,XNL,NU,F,T,U,SUM1)
DO 30 K=1,NU
IF(T(K))4,4,3
3 TEK=F(K)/(T(K)*DELT*SUM1)
GO TO 5
4 TEK=0.0
5 ULEV=U(K)
30 PRINT 150,TEK,ULEV,RH,Z,LAGS
GO TO 1
100 FORMAT(1H1,12X,7HMINIMAX,8X,5HLEVFL,8X,5HG-AMP,6X,5HG-LAG,4X,6HZER
IGES//)
150 FORMAT(6X,F16.8,5X,F5.3,6X,F7.3,5X,F6.3,5X,15)
200 FORMAT(F10.5,F5.3,15,F5.3,15)
220 FORMAT(15,F5.3,15)
230 FORMAT(4E16.8)
240 FORMAT(15)
999 STOP
END
```

A. Identification

Title: Subroutine INPUT

Programmer: Merdler

Date: March 1964

B. Purpose

To generate a synthetic seismogram.

C. Usage

1. Calling Sequence: Call INPUT (S, NS, RH, LAGG)
Uses library functions SETRND, RANDF, and SAVRND
stored in the PSU IBM 7074.

2. Arguments or parameters

S	synthetic seismogram
NS	number of points in synthetic signal
RH	ghost amplitude
LAGG	ghost delay time built into synthetic

3. Space required: Approximately 2500 locations

4. Input and Output Formats

a) Input

NS	number of points in primary reflectivity function
LAGG	built-in ghost delay time
LAGB	band-limiting filter delay time (usually zero)
RH	ghost amplitude (negative floating point number)
N	starting random number for RANDF
R	noise to signal power ratio

Format (4I5, F5.3, I20, F10.5)

S(I)	input primary reflectivity function
BLIM(I)	band-limiting filter

Format (7F10.5) for both

b) Output

S(I)	synthetic seismogram (4E16.8)
NS	number of points in synthetic
N	final random number generated (I20)

D. Method or Algorithm

This program convolves the input primary function $S(I)$ with $BLIM(I)$ and measures the total power of $S(I)*BLIM(I)$. It then generates NS random numbers $RAND(I)$ and knowing R computes the weighting constant RN . Ghosts of amplitude $RH*S(I)$ are added to $S(I)$ with delay time $LAGG$. Finally the primary plus ghost synthetic is convolved with $BLIM(I)$ and $RN*RAND(I)$ is added to this filtered signal.

```

FOR SYNTHETIC SIGNALS
SUBROUTINE INPUT(S,NS,RH,LAGG)
DIMENSION RAND(500),S(500),G(1000),BLIM(50)
READ 100,N,NR,R,NB,LAGP
CALL SETRND(N)
DO 5 I=1,NR
5 RAND(I)=RANDF(2.0)-1.0
CALL SAVRND(N)
READ 200,LAGP,LAGG,RH
NS=NR*(LAGP+2)
DO 10 I=1,NS
10 S(I)=0.0
DO 20 I=1,NR
K=I+(I-1)*LAGP
L=K+LAGG+1
S(K)=RAND(I)
20 S(L)=S(L)+RH*RAND(I)
CALL SETRND(N)
DO 25 I=1,NS
25 RAND(I)=RANDF(2.0)-1.0
CALL SAVRND(N)
PRINT 300,N
SUM1=0.0
SUM2=0.0
DO 30 I=1,NS
SUM1=SUM1+(S(I))**2
30 SUM2=SUM2+(RAND(I))**2
RN=SQRT(R*SUM1/SUM2)
DO 40 I=1,NS
40 S(I)=S(I)+RN*RAND(I)
READ 400,(BLIM(I),I=1,NE)
CALL COSKIP(BLIM,S,NR,NS,LAGP,G,NG)
BIGX=0.0
DO 50 I=1,NG
IF(ABS(BIGX)-ABS(G(I)))45,50,50
45 BIGX=G(I)
50 CONTINUE
DO 60 I=1,NS
60 S(I)=G(I)/ABS(BIGX)
PUNCH 500,(S(I),I=1,NS)
100 FORMAT(I20,I5,F10.5,2I5)
200 FORMAT(2I5,F5.3)
300 FORMAT(I20)
400 FORMAT(7F10.5)
500 FORMAT(4E16.8)
RETURN
END

```

```
FOR EARTHQUAKE SEISMOGRAMS
SUBROUTINE INPUT(S,NS,RH,LAGG)
DIMENSION S(500)
READ 100,NS,LAGG,RH
READ 300,(S(I),I=1,NS)
BIGX=0.0
DO 10 I=1,NS
IF(ABSF(BIGX)-ABSF(S(I)))5,10,10
5 BIGX=S(I)
10 CONTINUE
DO 20 I=1,NS
20 S(I)=S(I)/ABSF(BIGX)
PUNCH 500,(S(I),I=1,NS)
100 FORMAT(2I5,F5.3)
300 FORMAT(15F5.1)
500 FORMAT(4E16.8)
RETURN
END
```

A. Identification

Title: Subroutine COSKIP

Programmer: Merdier and Watson

Date: January 1964

B. Purpose

To convolve two functions and eliminate multiplying zeroes by skipping.

C. Usage

1. Calling Sequence: Call COSKIP(F,S,NF,NS,LAGS,G,NG)

2. Arguments or Parameters

F	first function (inverse operator)
S	second function (input signal)
NF	number of points in first function
NS	number of points in second function
LAGS	spacing between points in inverse operator
G	deconvolved input signal
NG	number of points in G

3. Space required: Approximately 2000 locations

4. Input and Output Formats

Determined by main program MINIMAX

5. Method or Algorithm

$$G(I) = \sum_{I=i}^{NG} \sum_{\substack{\text{MIN}(L, \text{NF}) \\ \text{MAX}(1, M)}} S \left[I - (J-1) \cdot (\text{LAGS} + 1) \right] \cdot F(J)$$

where $L = 1 + (I-1) / (\text{LAGS} + 1)$

$M = (I - \text{NS}) / (\text{LAGS} + 1) + 1$

```
PROGRAM COSKIP
CONVOLVES TWO FUNCTIONS
ELIMINATES MULTIPLYING ZEROES BY SKIPPING
SUBROUTINE COSKIP(F,S,NF,NS,LAGS,G,NG)
DIMENSION F(50),S(500),G(1000)
NG=NS+NF+(NF-1)*LAGS-1
DO 10 I=1,NG
L=1+(I-1)/(LAGS+1)
KUP=XMINOF(L,NF)
M=(I-NS)/(LAGS+1)+1
B=(I-NS)/(LAGS+1)+1
IF(B-FLOATF(M))3,3,2
2 M=M+1
3 KLOW=XMAXOF(1,M)
G(I)=0.0
DO 10 J=KLOW,KUP
MS=I-(J-1)*(LAGS+1)
10 G(I)=G(I)+S(MS)*F(J)
RETURN
END
```

A. Identification

Title: Subroutine CONVOL

Programmer: Merdler

Date: March 1964

B. Purpose

CONVOL convolves two functions using the COSKIP algorithm but does not store $G(I)$.

C. Usage

1. Calling Sequence

Call CONVOL (F, S, NF, NS, LAGS, XNL, NU, E, T, U, SUM1)

2. Arguments or parameters

F, S, NF, NS, LAGS same as for COSKIP

XNL, NU, U defined in main program

E, T, SUM1 are used in subroutine MINMAX

3. Space required: Approximately 600 locations

4. Input and Output Formats

Determined by main program MINIMAX

D. Method or Algorithm

Same algorithm used by COSKIP

A. Identification

Title: Subroutine MINMAX

Programmer: Merdler

Date: February 1964

B. Purpose

To compute the normalized percentage of energy of the filtered signal $G(I)$ above a specified u -level per unit of time.

C. Usage

1. Calling Sequence: Call MINMAX(G,XNL,NU,E,T,U,SUM1)

2. Arguments or parameters

G filtered signal (deconvolved input signal)
 E energy of ABSF(F(I)) for $G(I) > u$
 T total time width of ABSF(F(I)) for $G(I) > u$
 SUM1 total energy of ABSF(G(I)) for u -level = 0

XNL,NU,U defined in main program MINIMAX

3. Space required: Approximately 900 locations

4. Input and Output Formats

Determined by main program MINIMAX

D. Method or Algorithm

$$\text{TEK}(I,J) = \frac{\sum_{I=1}^T [\text{ABSF}(G(I)) - U(J)]^2}{T \cdot \text{DELT} \cdot \sum_{I=1}^{NG} [\text{ABSF}(G(I))]^2} \quad J = 1, 2, \dots, NU$$

where T = total number of $G(I)$ 'S for which $\text{ABSF}(G(I)) \geq U(J)$.

```

PROGRAM CONVOL
CONVOLVES TWO FUNCTIONS
ELIMINATES MULTIPLYING ZEROS BY SKIPPING
NO STORAGE OF OUTPUT
SUBROUTINE CONVOL(F,S,NF,NS,LAGS,XNL,NU,E,T,U,SUM1)
DIMENSION F(50),S(500),U(100),E(100),T(100)
NG=NS+NF+(NF-1)*LAGS-1
DO 20 I=1,NG
L=1+(I-1)/(LAGS+1)
KUP=XMINOF(L,NF)
M=(I-NS)/(LAGS+1)+1
B=(I-NS)/(LAGS+1)+1
IF(B-FLOATF(M))3,3,2
2  M=M+1
3  KLOW=XMAXOF(1,M)
G=0.0
DO 10 J=KLOW,KUP
MS=I-(J-1)*(LAGS+1)
10  G=G+S(MS)*F(J)
CALL MINMAX(G,XNL,NU,E,T,U,SUM1)
20  CONTINUE
RETURN
END

```

```

SUBROUTINE MINMAX(G,XNL,NU,E,T,U,SUM1)
MINMAX COMPUTES THE NORMALIZED PERCENTAGE OF ENERGY
OF THE FILTERED SIGNAL G(I) ABOVE A
SPECIFIED LEVEL U PER UNIT OF TIME
DIMENSION F(50),S(500),U(100),E(100),T(100)
SUM1=SUM1+G**2
DO 5 I=1,NU
U(I)=XNL*FLOATF(I)
DELTA=ABSF(G)-U(I)
IF(DELTA)8,8,6
6  E(I)=E(I)+DELTA**2
5  T(I)=T(I)+1.0
8  RETURN
END

```

A. Identification

Title: Executive Program OUTPUT

Programmer: Merdler

Date: February 1964

B. Purpose

Coordinates the functions of subroutines COSKIP and PLOTM for visual display of the correct inverse operator, input signal and filtered input.

C. Usage

1. Calling Sequence

None. This is a main program

2. Space required: approximately 3000 locations

3. Input and Output Formats

a) Input

NF	number of points in inverse operator
NS	number of points in input signal
LAGS	theoretical ghost delay time
LAGF	inverse operator lag
RH	ghost amplitude
DELT	input signal sampling increment
R	noise to signal power ratio
LAGG	actual ghost delay time
SCALE	plotting scale for subroutine PLOTM

Format (4I5, 2F5.3, F10.3, I5, F5.3)

F(I)	inverse operator	4E16.8
S(I)	input signal	4E16.8

b) Output

Printer

Values for NF, R, RH, LAGF

Values for NS, DELT, LAGG

Curves for F(I), S(I), F(I)*S(I), RH*(F(I)*S(I))
and F(I)*S(I)/(1+RH)

Printed using PLOTM

```

PROGRAM OUTPUT FOR SYNTHETIC SIGNALS
DIMENSION F(50),S(500),G(1000),H(500),E(500),GRAPH(20)
1 READ 50,NF,NS,LAGS,LAGF,RH,DELT,R,LAGG,SCALE
  IF(NF)999,999,2
2 READ 100,(F(I),I=1,NF)
  READ 100,(S(I),I=1,NS)
  CALL COSKIP(F,S,NF,NS,LAGS,G,NG)
  DO 10 K=1,NS
    MS=(LAGF-1)*(LAGS+1)+K
    LS=MS+LAGS+1
    H(K)=RH*G(MS)
10 E(K)=G(LS)+H(K)
  PRINT 300,NF,R,RH,LAGF
  PRINT 310
  CALL PLOTM(NF,F,SCALE)
  PRINT 400,NS,DELT,LAGG
  PRINT 310
  CALL PLOTM(NS,S,SCALE)
  PRINT 500
  PRINT 310
  CALL PLOTM(NG,G,SCALE)
  PRINT 600
  PRINT 310
  CALL PLOTM(NS,H,SCALE)
  PRINT 700
  PRINT 310
  CALL PLOTM(NS,E,SCALE)
  GO TO 1
50 FORMAT(4I5,2F5.3,F10.3,I5,F5.3)
100 FORMAT(4E16.8)
300 FORMAT(1H1,3HNF=,15,2X,2HR=,F7.5,2X,3HRH=,F7.3,2X,5HLAGF=,I5//1H
  122HOPTIMUM INVERSE FILTER/1H ,4HF(I),4X,9HTIME(SEC))
310 FORMAT(1H ,20X,4H-1,0,15X,4H-0,5,17X,3H0,0,17X,3H0,5,17X,3H1,0/
  123X,1HT,18X,1HT,19X,1HT,19X,1HT,19X,1HT)
400 FORMAT(1H0,3HNS=,15,2X,5HDELT=,F5.3,1X,3HSEC,1X,10HGHOST LAG=,I5/
  11H ,12HINPUT SIGNAL/1H ,4HS(I),4X,9HTIME(SEC))
500 FORMAT(1H0,14HFILTERED INPUT/1H ,4HG(I),4X,9HTIME(SEC))
600 FORMAT(1H0,12HGHOSTS ALONE/1H ,4HH(I),4X,9HTIME(SEC))
700 FORMAT(1H0,26HFILTERED INPUT PLUS GHOSTS/
  11H ,4HE(I),4X,9HTIME(SEC))
999 STOP
  END

```

```

PROGRAM OUTPUT FOR E=QUAKE DATA
DIMENSION F(50),S(500),G(4000),GRAPH(20)
1 READ 50,NF,NS,LAGS,LAGF,RH,DELT,R,LAGG,SCALE
  IF(NF)999,999,2
2 READ 100,(F(I),I=1,NF)
  READ 100,(S(I),I=1,NS)
  CALL COSKIP(F,S,NF,NS,LAGS,G,NG)
  PRINT 300,NF,R,RH,LAGF
  PRINT 310
  CALL PLOTM(NF,F,SCALE)
  PRINT 400,NS,DELT,LAGG
  PRINT 310
  CALL PLOTM(NS,S,SCALE)
  PRINT 300
  PRINT 310
  CALL PLOTM(NG,G,SCALE)
  GO TO 1
50 FORMAT(4I5,2F5.3,F10.3,I5,F5.3)
100 FORMAT(4E16.8)
300 FORMAT(11H1,3HNF=,I5,2X,2HR=,F7.5,2X,3HRH=,F7.3,2X,5HLAGF=,I5//1H ,
122HOPTIMUM INVERSE FILTER/1H ,4HF(I),4X,9HTIME(SEC))
310 FORMAT(1H ,20X,4H-1.0,15X,4H-0.5,17X,3H0.0,17X,3H0.5,17X,3H1.0/
123X,1HT,18X,1HT,19X,1HT,19X,1HT,19X,1HT)
400 FORMAT(1H0,3HNS=,I5,2X,5HDELT=,F5.3,1X,3HSEC,1X,10HGHST LAG=,I5/
11H ,12HINPUT SIGNAL/1H ,4HS(I),4X,9HTIME(SEC))
500 FORMAT(1H0,14HFILTERED INPUT/1H ,4HG(I),4X,9HTIME(SEC))
999 STOP
END

```

A. Identification

Title: Subroutine PLOTM

Programmer: Merdler

Date: January 1964

B. Purpose

To plot any two dimensional array. The program normalizes the quantities involved prior to plotting. Vertical scale is chosen by user (width of graph).

C. Usage

1. Calling Sequence: Call PLOTM(K,YORD,S)
Uses library functions SCALEF and GRAPHF stored in the PSU IBM 7074.

2. Arguments or Parameters

K	number of points to be plotted	K < 2000
YORD	value of ordinate	
S	scale value (maximum width of curve	< 10 inches)

How to determine S:

Suppose we desire that the maximum width of our graph to be 4 inches. We know that the normalized values of YORD will range between ± 1.0 .

$$\text{Scale} = \frac{\text{Max YORD} - \text{Min YORD}}{\text{Graph width}} = 0.5.$$

In this case YORD will be plotted with an accuracy of 0.05 units.

3. Space required: Approximately 2000 locations

4. Input and Output Formats

a) Input

Determined by main program

b) Output

Printer

Values of YORD(I)

Number of point I

Asterisk for value YORD(I)

Format (IHS, F8.4, 3X, I5, 5X, 20A5)

5. Accuracy:

Values of YORD(I) may be plotted no closer than 0.01 units.

D. Method or Algorithm

Uses library functions SCALEF and GRAPHF written by Forney
(PSU programming consultant).

```
1 SUBROUTINE PLOTM(K,YORD,S)
2 DIMENSION GRAPH(20),YORD(2000)
3 BIGX=0.0
4 DO 7 I=1,K
5 IF(ABSF(BIGX)-ABSF(YORD(I)))6,7,7
6 BIGX=YORD(I)
7 CONTINUE
8 DO 9 I=1,K
9 YORD(I)=YORD(I)/ABSF(BIGX)
10 DO 14 I=1,K
11 D=SCALEF(-1.0,S)
12 DUMMY=GRAPHF(GRAPH,YORD(I),1H*)
13 PRINT 100,YORD(I),I,GRAPH
14 CONTINUE
15 PRINT 200,BIGX
100 FORMAT(1HS,F8.4,3X,I5,5X,20A5)
200 FORMAT(1H ,21H NORMALIZING FACTOR =,F10.4)
16 RETURN
17 END
```

REFERENCES

- Birch, F., J. F. Schairer and H. C. Spicer (1942) Handbook of Physical Constants, Geo. Soc. Am. Sp. Paper, 36.
- Bogert, B. P., M. R. J. Healy and J. W. Tukey (1963) The quefrequency analysis of time series for echoes: cepstrum, pseudo-auto-covariance, cross-cepstrum and saphe cracking: Ch. 15, 209-243 of Rosenblatt, 1963.
- California Research Corp. (1961) Semi-annual technical report No. 1, ARPA Contract AF19(603)-8344.
- Churchill, R. V. (1958) Operational Mathematics, McGraw-Hill Book Company, New York.
- De Bremaecker, J. C. (1955) Use of Amplitudes, Part II, Focal Depths: Bull. Seis. Soc. Am., 45, 279-284.
- Foster, M. R., W. G. Hicks and J. T. Nipper (1962) Optimum inverse filters which shorten the spacing of velocity logs: Geophysics, 27, 317-326.
- Foster, M. R., R. L. Sengbush and R. J. Watson (1964) Design of sub-optimum filter systems for multitrace seismic data processing: Geophysical Prospecting, 12 (in press).
- Gunst, R. H. and E. R. Engdahl (1962) Progress report of USC&GS hypocenter computer program: Earthquake Notes, 23, 93-96.
- Gutenberg, B. (1955) Wave velocities in the earth's crust: Geol. Soc. Am. Sp. Paper, 62.
- Gutenberg, B. (1958) Wave velocities below the Mohorovicic discontinuity: The Geophysical Journal, 1, 351.
- Howell, B. F., Jr. (1959) Introduction to Geophysics, McGraw-Hill Book Company, New York.
- Howell, B. F., Jr., P. M. Lavin and R. J. Watson (1963) Studies of the effect of depth of focus on seismic pulses: Fourth Semi-Annual Report, ARPA Contract AF19(628)-235.
- Jeffreys, H. and K. E. Bullen (1940) Seismological Tables, London Office of the British Association Burlington House, W.1.

- Keylis Borok, V. I. (1962) Seismic effects of underground explosions: Differences in the spectra of surface waves from earthquakes and explosions: New York Consultants Bureau.
- Kondorskaya, N. V. (1965) Identification of the sP wave in shallow earthquakes and its use in determining the depth of focus: Akad. Nauk SSSR Geof. Inst. Trudy, 36, 35-37
- Lee, Y. W. (1963) Statistical Theory of Communication, John Wiley and Sons, Inc., New York.
- Lindsey, J. P. (1960) Elimination of ghost reflections by means of a linear filter: Geophysics, 25, 130-140.
- Nakamura, Y. (1963) Frequency spectra of refraction arrivals and the nature of the Mohorovicic discontinuity: Ph.D. Thesis, Department of Geology and Geophysics, The Pennsylvania State University.
- Nuttli, O. W. and J. D. Whitmore (1961) An observational determination of the angle of incidence of P waves with epicentral distance: Seismol. Soc. America Bull., 51, 269-276.
- Peterson, R. A., W. R. Fillipone and F. B. Coker (1955) The synthesis of seismograms from well-log data: Geophysics, 20, 516-538.
- Rosenblatt, M. (1963) Time Series Analysis, John Wiley and Sons, Inc., New York.
- Rothman, R. L. (1964) Model studies for focal depth determination at near-source stations: M. S. Thesis, Department of Geology and Geophysics, The Pennsylvania State University.
- Sengbush, R. L., P. L. Lawrence and F. J. McDonal (1961) Interpretation of synthetic seismograms: Geophysics, 26, 138-157.
- Simpson, S. M. (1961) Time series techniques applied to underground nuclear detection and further digitized seismic data: Sci. Report 2, Air Force Contract (M.I.T.) 19(604)7378.
- Simpson, S. M., Jr. (1962) Numerical studies on underground nuclear detection and further digitized seismic data: June 30 report of ARPA Contract AF19(604)7378.
- Steinhart, J. S. and R. P. Meyer (1961) Explosion Studies of Continental Structure, Carnegie Institution of Washington Publication 622, Washington, D. C.
- Thirlaway, H. I. S. (1961) Depth of focus discrimination within the crust at first-zone distances: VESIAC Special Advisory Report Number 1, Institute of Science and Technology, The University of Michigan.

U. S. Department of Commerce Coast and Geodetic Survey (1964) Preliminary Determination of Epicenters, Special card number 1-64, Washington 25, D. C.

Weiner, N. (1949) Extrapolation, Interpolation and Smoothing of Time Series, John Wiley and Sons, Inc., New York.

The Pennsylvania State University, Dept. of Geology and Geophysics, University Park, Pa., ESTIMATION PROCEDURE FOR FOCAL-DEPTH DETERMINATION OF SEISMIC DISTURBANCES by S. C. Merdler. Air Force Cambridge Research Laboratories, Bedford, Mass. Special Technical Report - Number AFRL-64-755, 94 pages, September 1964.

Unclassified Report

A new data processing technique is suggested to estimate the delay time between initially uptraveling energy which is reflected once at the earth's surface and initially downtraveling energy on earthquake seismograms. The method uses optimum inverse filters together with a criterion that measures the simplicity of a seismic signal involved with an inverse filter. The inverse filters are designed to extract primary energy in the presence of surface reflected energy and random noise on the basis of a least-mean-square error criterion. Filter design is dependent on the delay time between primaries and surface reflected events, their amplitude ratio and noise to signal power ratio. The simplicity criterion was devised on the assumption that a maximum in the concentration of normalized seismic signal energy above a minimum level indicates which filter was most correctly designed. This is visualized as an expression of the hypothesis that the primary seismogram is generated by a few large discontinuities, rather than by many minor boundaries.

The method was tested on synthetic signals and four earthquake seismograms. It is concluded that it provides a reasonable estimate of delay time between primary and surface-reflected energy.

1. Depth of focus of a seismic disturbance
2. Original shape of a seismic pulse

- I. Project No. 8652
Task No. 865208
- II. Contract AFL9(628)-238
- III. S. C. Merdler
- IV. In DDC collection